land

MDPI

Article

Spatiotemporal Dynamics and Driving Mechanisms of Ecosystem Services in the Beijing–Tianjin–Hebei Urban Agglomeration: Implications for Sustainable Land Use Planning

Shuanqging Sheng [1,2] and Jinchuan Huang [1,*]

[1] Key Laboratory of Regional Sustainable Development Modeling, Institute of Geographic Sciences and Natural Resources Research, Chinese Academy of Sciences, Beijing 100101, China; shengsq@cau.edu.cn
[2] College of Land Science and Technology, China Agricultural University, Beijing 100193, China
* Correspondence: huangjc@igsnrr.ac.cn

Abstract: The accelerating process of global urbanization has substantially reshaped land use patterns, exerting profound influences on the dynamics of ecosystem service provision. Effective and adaptive ecosystem management necessitates the quantitative identification and analysis of spatiotemporal variations in ecosystem services and their underlying driving mechanisms. Using the Beijing–Tianjin–Hebei urban agglomeration as a case study, this research examines land use dynamics from 2000 to 2020 and projects land use patterns for 2030 under alternative development scenarios. Building upon this foundation, the study quantifies the spatiotemporal evolution of four key ecosystem services—Carbon Storage (CS), Water Yield (WY), Habitat Quality (HQ), and Soil Retention (SDR)—from 2000 to 2030, while elucidating the differential impacts and underlying mechanisms of the driving factors on these services. The findings indicate that: (1) Between 2000 and 2020, cultivated land remained the dominant land use type (47.71%), followed by forestland (21.44%) and grassland (16.23%), whereas built-up land expanded significantly from 8.12% to 12.74%; (2) the proportion of medium-to-high CS areas reached 47.65%, high-value WY areas increased by 4.9%, low-value HQ areas expanded by 4.28%, and low-value SDR areas accounted for 84.44%; (3) the PLUS model validation yielded a Kappa coefficient of 86.1%, indicating high simulation accuracy. Scenario-based predictions suggest that under an ecological protection scenario, the proportion of medium-to-high CS areas would increase by 0.59%, whereas under an economic development scenario, these areas would decline by 2.57%, with low-value HQ areas expanding by 2.04%; (4) slope (X_2) was identified as the dominant factor influencing CS (q = 0.22), HQ (q = 0.36–0.42), and SDR (q = 0.42), while mean annual precipitation (X_4) played a crucial role in determining WY. Furthermore, socioeconomic activities, particularly increasing population density, exhibited a growing negative impact on HQ and CS, highlighting the intensifying role of anthropogenic interventions in shaping ecosystem service patterns. This study unveils the spatial heterogeneity of ecosystem services and their driving mechanisms in the context of urbanization, offering valuable insights to inform regional ecological conservation and sustainable development policies.

Keywords: land use change; ecosystem services; scenario simulation; driving factors; Beijing–Tianjin–Hebei urban agglomeration

check for updates

Academic Editor: Shiliang Liu

Received: 18 March 2025
Revised: 23 April 2025
Accepted: 27 April 2025
Published: 30 April 2025

Citation: Sheng, S.; Huang, J. Spatiotemporal Dynamics and Driving Mechanisms of Ecosystem Services in the Beijing–Tianjin–Hebei Urban Agglomeration: Implications for Sustainable Land Use Planning. *Land* **2025**, *14*, 969. https://doi.org/10.3390/land14050969

Copyright: © 2025 by the authors. Licensee MDPI, Basel, Switzerland. This article is an open access article distributed under the terms and conditions of the Creative Commons Attribution (CC BY) license (https://creativecommons.org/licenses/by/4.0/).

1. Introduction

Ecosystem services (ES) encompass the diverse benefits that humans derive from natural ecosystems, forming a fundamental basis for human survival and sustainable

development while holding substantial ecological and socioeconomic value [1,2]. However, land use change, as a predominant manifestation of anthropogenic activities, exerts profound influences on the supply capacity and spatial configuration of ecosystem services [3]. From a direct impact perspective, the conversion of land use types and the restructuring of spatial patterns significantly reshape ecosystem service provision. For instance, urban expansion and agricultural development encroach upon natural ecosystems, diminishing critical functions such as soil retention and water purification, while intensifying trade-offs among ecosystem services, ultimately leading to ecosystem degradation [4]. Indirectly, land use change exacerbates habitat fragmentation and disrupts landscape connectivity, thereby weakening ecosystem stability and adversely affecting human well-being [5,6]. Extensive research indicates that global industrialization and urbanization have led to the degradation of approximately 60% of ecosystem services (flood mitigation, crop pollination, and nature-based recreation), posing a significant threat to the sustainability of human societies [7]. The Millennium Ecosystem Assessment (MA) further underscores that excessive exploitation of ecosystems is accelerating the decline of essential ecosystem functions, thereby compromising regional ecological security and impeding progress toward global sustainable development goals [8]. Therefore, an in-depth exploration of the interaction mechanisms between land use change and ecosystem services is crucial for informing ecosystem conservation strategies, optimizing service functions, and enhancing human well-being.

In recent years, the field of ecosystem services has witnessed substantial advancements across methodological frameworks, research foci, and data utilization. Methodologically, the extensive application of quantitative tools—such as the equivalent factor method, ARIES, and InVEST models—has significantly improved the capacity to capture and quantify the spatiotemporal dynamics of ecosystem services [9]. Regarding research content, scholarly attention has progressively shifted from the isolated assessment of single services (e.g., carbon sequestration, habitat quality) toward the development of ecological risk assessment frameworks within the context of land use change [10]. Research priorities have likewise evolved, increasingly emphasizing the spatial heterogeneity of ecosystem services, the trade-offs and synergies among multiple services, and the spatial alignment of ecosystem service supply and demand [11,12]. On the data side, relevant studies have made extensive use of historical and current land use datasets, socioeconomic statistics, and spatially explicit grid data to support multiscale ecosystem service analyses [13]. As the research landscape deepens, ecosystem services are increasingly conceptualized as an integrated multifunctional system, wherein complex trade-offs and synergistic interactions occur among various service types. Consequently, single-function evaluations are no longer sufficient to inform territorial spatial optimization and ecological management strategies. Comprehensive assessments of multiple ecosystem services, grounded in a systems-thinking perspective, have thus emerged as a critical research frontier. Recent studies have sought to identify representative service bundles, investigate their spatiotemporal trajectories and underlying drivers, and elucidate the interactions and spatial coupling among services. Nevertheless, the existing literature remains predominantly retrospective in orientation, with limited exploration of the dynamic responses of ecosystem services to divergent future land use scenarios. In practice, the evolution of ecosystem services is shaped by a complex interplay of biophysical, socioeconomic, and institutional factors, and is inherently dynamic and uncertain [14]. Although retrospective analyses of past policy impacts have yielded valuable insights, the capacity for regional-scale dynamic simulation of ecosystem services under multiple future scenarios remains insufficiently developed. This gap constrains the depth and scope of ecosystem service research in supporting spatial planning and policymaking. Hence, future research should prioritize

the integration of scenario-based simulations with multiservice assessments to enhance the practical relevance and decision-support capacity of ecosystem service evaluations.

Scenario analysis, as a prospective research methodology, serves as a vital instrument for forecasting potential changes in ecosystem services under alternative land use trajectories, thereby offering a scientific basis for regional spatial planning and ecological conservation decision-making [15]. At the modeling level, spatial simulation approaches such as Cellular Automata (CA), the Conversion of Land Use and its Effects at Small regional extent (CLUE-S) model, and the Patch-level Land Use Simulation Model (PLUS) have proven effective in predicting land use change patterns across different scenarios, thereby providing critical baseline data for the quantitative evaluation of ecosystem services [15–17]. These models play a crucial role in assisting planners in identifying optimal resource conservation strategies, enhancing spatial configurations, and promoting efficient land resource allocation. Nevertheless, considerable variation exists among models in terms of their performance and applicability. The CLUE-S model is particularly well-suited for simulating land use changes at small regional scales, whereas the PLUS model—anchored in cellular automata theory—offers higher simulation precision and enhanced capability at the patch level, rendering it more appropriate for addressing complex land use dynamics [16,17]. With respect to scenario design, studies commonly employ logically coherent and internally consistent assumptions or narrative frameworks to characterize the spatiotemporal evolution of land use/land cover and its driving forces [18]. This methodological framework not only enhances the scientific robustness and interpretability of ecosystem service quantification, but also provides a foundation for the development of resilient land use policy strategies [18]. Accordingly, the judicious selection of simulation models and the systematic construction of scenario narratives are central to advancing land use change simulation research. A pressing research need lies in the ability to quantify the impacts of land use transitions on ecosystem services under divergent development scenarios, thereby supporting more informed and sustainable territorial spatial planning.

The identification and quantification of the driving forces behind ecosystem services are critical for informing evidence-based natural resource management strategies. Recent studies have made incremental progress in uncovering the underlying driving mechanisms. For example, some investigations have utilized qualitative methods to examine the impacts of policy interventions and socioeconomic dynamics on ecosystem services, drawing upon quantified service values as the analytical foundation [19]. Additionally, studies utilizing structural equation modeling (SEM) have quantified the relationships between ecosystem services, human demand, and well-being [20]. The Random Forest Model has also been employed in ecosystem service modeling across various regions, integrated with Shapley Additive Explanations (SHAP) to uncover underlying driving mechanisms [21]. Despite these advancements, there remains a gap in the literature. Primarily, much of the existing research emphasizes qualitative analysis, lacking detailed, geographically informed quantitative comparisons and in-depth explorations [22]. Furthermore, ecosystem services are influenced by the complex and intertwined interactions among natural, economic, and social factors, underscoring the need for a comprehensive indicator system to fully elucidate the mechanisms underlying these drivers—an ongoing scientific challenge [23]. The Geographical Detector method provides a reliable approach for revealing the driving factors of ecosystem services [24]. Rooted in the principle of spatial differentiation, this method effectively identifies the causes of spatial heterogeneity in ecosystem services, while also elucidating the interactions between multiple influencing factors [25]. Therefore, the Geographical Detector offers a critical quantitative tool for the comprehensive analysis of the driving mechanisms underlying ecosystem services.

As one of China's most densely populated, economically vibrant, and urbanized regions, the Beijing–Tianjin–Hebei (BTH) area has long been confronted with increasing pressures on resources and the environment, as well as a significant imbalance between the supply and demand of ecosystem services. In recent years, the deepening implementation of the BTH coordinated development strategy has led to marked shifts in regional land use patterns. These ongoing adjustments have notably altered the spatial distribution and supply capacity of ecosystem services, while simultaneously presenting new challenges in ecological conservation and resource allocation. Driven by the dual objectives of carbon reduction and territorial spatial optimization, a detailed investigation into the spatiotemporal dynamics and underlying drivers of ecosystem services under various land use scenarios is essential. Such an analysis will not only aid in the identification of highly sensitive areas and critical influencing factors, but will also provide valuable theoretical insights and practical support for the development of regional ecological security frameworks and enhanced territorial governance.

In this context, the study aims to achieve the following objectives: (1) to analyze the spatiotemporal patterns and evolutionary trends of land use change in the BTH region from 2000 to 2020; (2) to quantify the dynamic changes and spatial differentiation of total ecosystem services in the study area under different development scenarios for the years 2000–2020 and 2030; and (3) to explore the impacts of natural geographic and socioeconomic factors on ecosystem services. This research seeks to provide scientific evidence to inform territorial spatial planning and optimize ecological security patterns in the Beijing–Tianjin–Hebei region.

2. Study Area and Data Sources

2.1. Overview of the Study Area

The Beijing–Tianjin–Hebei (BTH) region (36°05′—42°37′ N, 113°11′—119°45′ E), located in the heart of North China, is bordered by the Yanshan Mountains to the north, the Taihang Mountains to the west, and the Bohai Sea to the east. Often referred to as the "Capital Economic Circle" (Figure 1) [26], the region is comprised of Beijing, Tianjin, and eleven prefecture-level cities within Hebei Province, namely Baoding, Tangshan, Langfang, Qinhuangdao, Zhangjiakou, Chengde, Shijiazhuang, Cangzhou, Handan, Xingtai, and Hengshui, covering a total area of 218,000 km^2. The region exhibits a general northwest-to-southeast topographic gradient and is characterized by diverse landforms. Its climate is classified as temperate, semi-humid to semi-arid monsoon, with distinct seasonal variations: dry and windy conditions in spring and autumn, hot and rainy summers, and cold and dry winters. These varied natural conditions have provided substantial support for the region's economic development and population concentration.

In recent years, the BTH region has experienced accelerated urbanization, accompanied by a high concentration of both population and industrial activity. As of 2022, the region's permanent population reached 109.7 million, and by 2024, the gross regional product (GDP) is expected to total 11.539 trillion CNY, reflecting a year-on-year growth of 5.2%. The region plays a pivotal role in China's political, economic, and cultural landscape and is also an integral part of the national ecological security framework. However, rapid urban expansion and high-intensity economic activity have given rise to challenges such as ecological fragmentation and the degradation of ecosystem service functions. Therefore, identifying and analyzing the key drivers of land use change is essential for gaining a deeper understanding of the mechanisms behind the evolution of ecosystem services, enhancing ecological governance capacity, and optimizing land resource allocation.

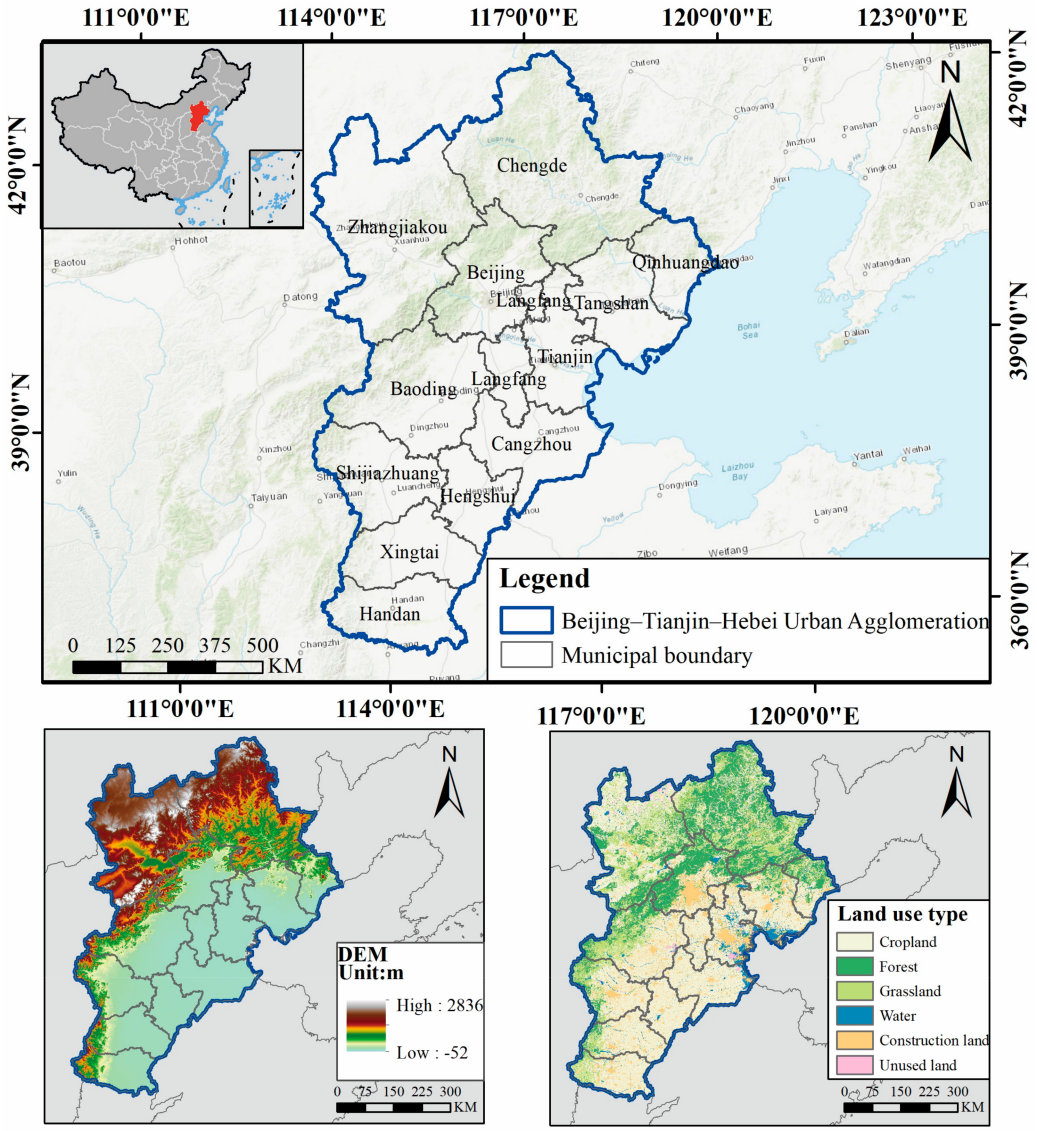


Figure 1. Overview of the study area.

2.2. Data Sources

The research data can be classified into three categories based on their respective applications (Table 1). The first category consists of land use status remote sensing monitoring data, primarily derived from Landsat satellite imagery, which has been interpreted using manual visual analysis to construct a multitemporal land use/land cover database at the national scale in China. This dataset is sourced from the Resource and Environment Science Data Center of the Chinese Academy of Sciences (http://www.resdc.cn, accessed on 8 December 2024), and it has been widely utilized in land use change analysis and dynamic simulation studies. Notably, the remote sensing imagery used in this database has a spatial resolution of 30 m, providing high spatial accuracy that supports regional-scale land use monitoring and assessment.

Table 1. Spatial resolution, source, and use of the data.

Data	Time	Resolution	Source	Purpose Description
Land Use Remote Sensing Monitoring Dataset	2000, 2010, 2020	30 m	Resource and Environmental Science Data Platform (https://www.resdc.cn/, accessed on 8 December 2024)	Analyze land use changes and simulate
Soil Data Source		-	World Soil Database (http://westdc.westgis.ac.cn/data/, accessed on 8 December 2024)	Quantify ecosystem services
Meteorological Data		-	Resource and Environmental Science Data Platform (https://www.resdc.cn/, accessed on 8 December 2024)	
DEM, Slope, Aspect		90 m	Resource and Environmental Science Data Platform (https://www.resdc.cn/, accessed on 8 December 2024)	
Annual Mean Temperature		1 km	Copernicus Publications [27]	
Annual Mean Precipitation		1 km	Copernicus Publications [27]	Analyze driving factors of ecosystem services and land use change simulation
Evaporation		1 km	Resource and Environmental Science Data Platform (http://www.resdc.cn/, accessed on 8 December 2024)	
NDVI		1 km	NASA [28]	
Population Density		1 km	Resource and Environmental Science Data Platform (https://www.resdc.cn/, accessed on 8 December 2024)	
GDP		1 km	Resource and Environmental Science Data Platform (https://www.resdc.cn/, accessed on 8 December 2024)	
Nighttime Light		1 km	Scientific Data [29]	

The second category comprises data essential for the quantification of ecosystem services, which primarily includes soil and meteorological data. Soil data is sourced from the World Soil Database (http://westdc.westgis.ac.cn/data/, accessed on 8 December 2024), which includes key soil properties such as sand, silt, and clay content, along with organic carbon content, at a spatial resolution of 1 km. This dataset is pivotal for quantifying carbon storage, habitat quality, and soil conservation services. Meteorological data, including annual precipitation and potential evapotranspiration, is obtained from the Resource and Environmental Science Data Platform (http://www.resdc.cn/, accessed on 8 December 2024). These data are crucial for estimating water yield and soil erosion and serve as critical drivers in regulating ecosystem water supply capacity and habitat stability.

The third category consists of data related to the driving factors of spatial ecosystem service evolution, which is primarily used to identify and investigate the influence mechanisms of various natural and human factors on ecosystem service patterns. The selection of these driving factors is informed by the ecological foundations and socioeconomic disturbance mechanisms involved in the formation of ecosystem services, adhering to the principles of scientific rigor, representativeness, and accessibility. Natural environmental factors include topographical features such as elevation, slope, and aspect, as well as climate factors such as annual precipitation, temperature, and evaporation. These factors directly influence regional water-heat conditions, vegetation growth potential, and soil erosion susceptibility, forming the natural basis for ecosystem service spatial distribution. Additionally, the Normalized Difference Vegetation Index (NDVI), which serves as a key remote sensing indicator of surface vegetation cover, is instrumental in characterizing regional ecological function variability, indirectly reflecting the spatial intensity of services such as carbon storage, habitat quality, and soil conservation.

From the perspective of socioeconomic factors, indicators such as population density, night-time light intensity, and gross regional product (GDP) are selected to capture the intensity of human activities and economic development levels. These factors influence the spatial evolution of ecosystem structure and service functions, particularly in rapidly urbanizing regions, where their impact on ecosystem service patterns is notably pronounced.

3. Research Design and Methodology

3.1. Research Design

This study initially constructs the spatiotemporal trajectories of ecosystem service evolution from 2000 to 2020, along with an analysis of their underlying driving mechanisms, thus providing an empirical foundation for simulating potential land-use scenarios for 2030. The scenario development is informed not only by policy documents, such as the "Beijing-Tianjin-Hebei Regional Land Spatial Planning", but also by historical trends in land-use transitions and shifts in dominant driving factors. To enhance the explanatory power of the model's simulation outcomes, this study further contrasts the 2030 ecosystem service projections with the key driving factors identified during previous phases, thereby investigating whether the simulated scenarios perpetuate or alter the established pathways of influence. This research aims to offer a comprehensive set of insights and policy recommendations to guide land, spatial optimization, and ecosystem service management.

In particular, the study employs remote sensing and GIS technologies to integrate a variety of data sources, including land use, climate, and ecosystem services, in order to quantify changes in land use, carbon storage, water production, habitat quality, and soil conservation—four essential ecosystem services. On this basis, three future scenarios for 2030 are proposed: an inertia-driven development scenario, an economic development scenario, and an ecological protection scenario. These scenarios are used to simulate the spatial distribution characteristics of ecosystem services under each respective condition. Lastly,

driving factors from both natural geographic and socioeconomic dimensions are selected to explore their influence mechanisms on ecosystem services. The research framework is illustrated in Figure 2.

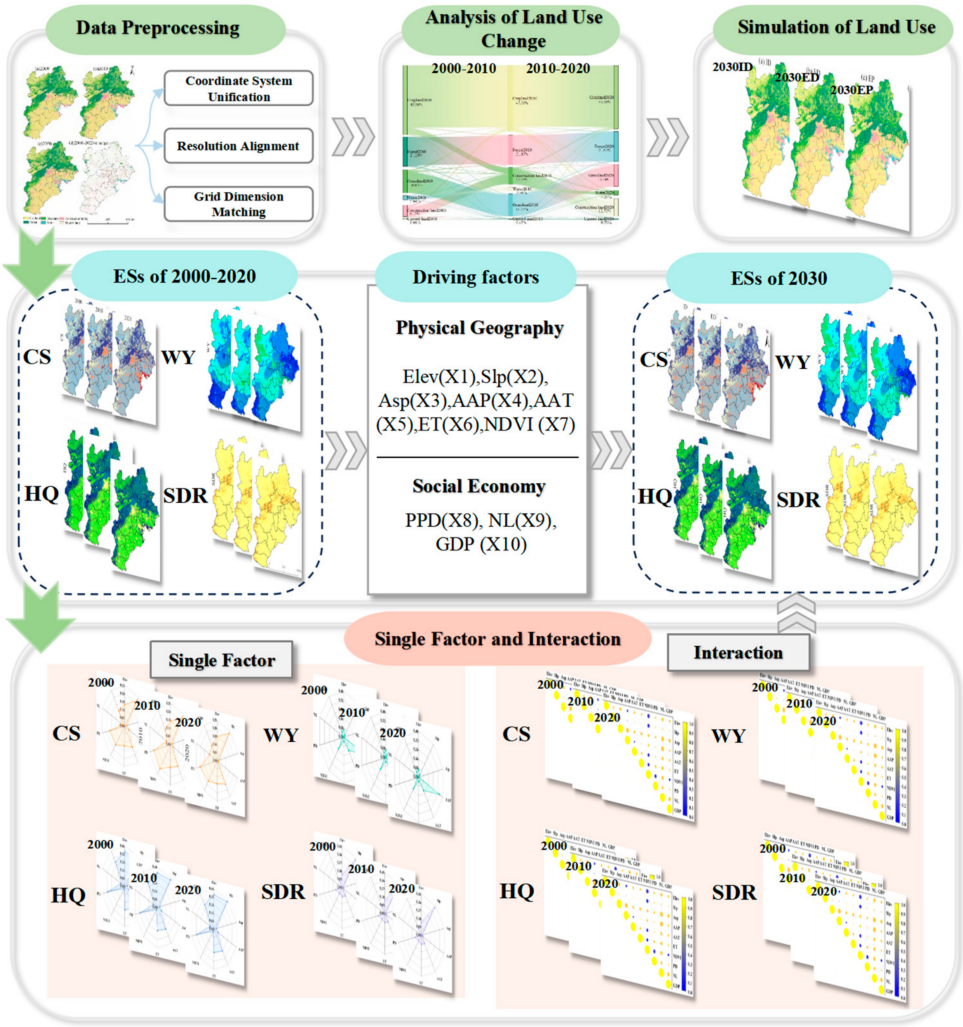


Figure 2. Technical framework. Note: CS represents Carbon Storage, WY represents Water Yield, HQ represents Habitat Quality, SDR represents Soil Retention Service, Elev represents Elevation (X_1), Slp represents Slope (X_2), Asp represents Aspect (X_3), AAP represents Annual Average Precipitation (X_4), AAT represents Annual Average Temperature (X_5), ET represents Evapotranspiration (X_6), NDVI represents the Normalized Difference Vegetation Index (X_7), PD represents Population Density (X_8), NL represents Nighttime Light (X_9), and GDP represents Gross Domestic Product (X_{10}).

3.2. Land Use Transition Matrix

The land use transition matrix provides a clear depiction of the interrelationships among different land use types, encompassing information such as sources, destinations, and the areas of transition. In this study, the land use transition matrix method is employed to analyze the dynamic land use changes in the Beijing–Tianjin–Hebei region from 2000 to 2020. Using a decadal interval, the study primarily focuses on examining the transition structure and spatial transformation directions of various land types at both the beginning and end of the study period [30]. Its calculation formula is as follows:

$$A = (A_{ij})_{n\times n} = \begin{bmatrix} A_{11} & \cdots & A_{1n} \\ \vdots & \ddots & \vdots \\ A_{n1} & \cdots & A_{nn} \end{bmatrix} \quad (1)$$

The variable A represents the area of each land use type, while n denotes the total number of land use types. The indices i and j correspond to the land use types at the start and end of the study period, respectively, with A_{ij} indicating the area of land type i transitioning to land type j over the study period. Utilizing land use data from both time periods, the land use transition matrix is derived through spatial overlay analysis conducted with ArcGIS 10.8 software, facilitating an analysis of the dynamic evolution of land use types.

3.3. Ecosystem Service Assessment

The quantification of ecosystem services offers a systematic approach to evaluating the contributions of ecosystems to human well-being and constitutes a vital foundation for ecological protection and regional sustainable development [9]. As a process-driven tool, the InVEST model facilitates the quantification of multiple ecosystem functions and their potential economic values, thereby providing scientific support for ecosystem management and land use planning [9]. In recent years, the implementation of regional integration strategies has led to marked transformations in land use patterns across the Beijing–Tianjin–Hebei region, significantly reshaping the spatial provisioning capacity of ecosystem services and revealing pronounced spatial heterogeneity driven by disparities in natural geography and socioeconomic development.

Given the region's diverse topography, pronounced climatic gradients, and accelerated urbanization, this study conducts a quantitative assessment of four representative ecosystem services—carbon storage, water yield, habitat quality, and soil retention—encompassing provisioning, regulating, and supporting functions. By coupling ecosystem service evaluations with land use change trajectories, the study investigates the underlying mechanisms driving the spatial dynamics of ecosystem services, with the aim of providing a scientific basis for integrated ecological governance and the promotion of high-quality development in the Beijing–Tianjin–Hebei region.

3.3.1. Carbon Storage

Carbon storage refers to the capacity of ecosystems to absorb and sequester atmospheric carbon dioxide via photosynthesis, subsequently storing it in biomass and soils. The carbon storage module of the InVEST model is employed to quantify the role of ecosystems in carbon sequestration, typically encompassing four primary carbon pools: aboveground biomass, belowground biomass, soil organic carbon, and dead organic matter. In this study, the habitat quality module of the InVEST model is applied to quantify regional carbon storage by integrating land use data with the parameters of these carbon pools, thus assessing the carbon sequestration potential of the Beijing–Tianjin–Hebei region [31]. Its calculation formula is in Appendix A.1.

3.3.2. Water Yield

Water yield refers to the capacity of ecosystems to generate usable water resources for human consumption through processes such as precipitation interception, soil infiltration, and water retention. The water yield module of the InVEST model is based on the Budyko water-energy balance framework and incorporates the soil permeability and evapotranspiration characteristics of different land use types to quantitatively estimate the region's annual water yield [31]. In this study, the module is applied to compute the difference between annual average precipitation and actual evapotranspiration, providing a measure of water yield in the Beijing–Tianjin–Hebei region. This approach further reveals the spatial distribution patterns and ecological regulation functions of water yield. Its calculation formula is in Appendix A.2.

3.3.3. Habitat Quality

Habitat quality refers to an ecosystem's capacity to provide a suitable living environment for species, encompassing both habitat integrity and the risks faced by species within these habitats. The habitat quality module of the InVEST model quantifies the impacts of threat factors on habitat conditions by calculating the Habitat Risk Index (HRI) and producing a spatial distribution map of habitat quality. In this study, the module is applied by integrating land cover data with biodiversity threat factors to produce spatial raster data representing habitat quality. This method enables the quantification of habitat conditions and their spatial variation across the Beijing–Tianjin–Hebei region [31]. Its calculation formula is in Appendix A.3.

3.3.4. Soil Retention Service

Soil retention refers to the capacity of ecosystems to mitigate soil erosion and degradation through mechanisms such as vegetation cover, root stabilization, and improvements in soil structure. The soil retention module of the InVEST model is based on the Revised Universal Soil Loss Equation (RUSLE) and the Sediment Delivery Ratio (SDR) module. It quantifies soil retention by calculating the difference between potential and actual soil erosion under natural vegetation cover. In this study, the module is applied in conjunction with land use, climate, soil, and topographic data from the study area to conduct a spatially explicit and quantitative analysis of soil retention services. This approach reveals the spatial distribution characteristics of soil retention functions within the Beijing–Tianjin–Hebei region [31]. Its calculation formula is in Appendix A.3.

3.4. Land Use Multiscenario Simulation

3.4.1. The PLUS Model and Accuracy Verification

(1) PLUS Model

The PLUS model, an enhancement of the FLUS model, offers superior capabilities for analyzing the driving forces behind land use change, enabling fine-scale patch-level simulations that surpass traditional geographic cellular automata approaches. This model integrates a multiobjective optimization algorithm, which combines a land expansion strategy analysis module with a cellular automaton that utilizes random patch seeds. The former extracts land expansion data, while the latter employs a random seed generation mechanism and a threshold decrement process to facilitate the dynamic spatiotemporal simulation of land use patches [32].

(2) Selection of Driving Factors

This study establishes a driving factor system that integrates both natural environmental characteristics and socioeconomic development within the Beijing–Tianjin–Hebei region. The system incorporates ten indicators: elevation, slope, aspect, annual precipitation, annual temperature, evapotranspiration, NDVI, population density, nighttime light intensity, and GDP, each selected for its distinct ecological relevance and spatial responsiveness.

Regarding natural factors, topographic variables (elevation, slope, aspect) influence land accessibility and suitability, significantly shaping the spatial distribution of agricultural and construction lands, particularly in mountainous and hilly areas where their constraining effects are most evident. Climatic factors (annual precipitation, annual temperature, and evapotranspiration) provide a comprehensive understanding of the region's water-heat conditions, substantially affecting vegetation growth and agricultural land patterns. NDVI, as a sensitive indicator of vegetation cover, reflects both ecological quality and the intensity of human-induced disturbances, offering crucial insights into changes in ecologically sensitive areas.

From a socioeconomic perspective, population density, night-time light intensity, and GDP capture the intensity of human activity from the dimensions of population concentration, spatial development, and economic growth, respectively. These factors serve as key drivers of urban land expansion. Specifically, night-time light intensity, recognized as a precise proxy for urbanization, has demonstrated strong adaptability and explanatory power in modeling urban expansion across diverse regions.

Existing literature suggests that a driving factor system encompassing both natural and anthropogenic elements enhances the accuracy and stability of land-use change simulations, particularly in regions characterized by rapid urbanization and complex topographies. Consequently, the selection of driving factors in this study is both theoretically robust and empirically supported, providing a sound basis for simulating land-use changes in the Beijing–Tianjin–Hebei region by 2030.

(3) Accuracy Validation

In land use change modeling, the Kappa coefficient is a statistical indicator commonly used to measure the agreement between simulated results and actual observations. It is widely employed in the evaluation of model accuracy. In this study, the 2010 land use data for the Beijing–Tianjin–Hebei region serves as the reference to validate the accuracy of the PLUS model and to predict the land use scenario for 2020. By comparing the simulated and observed data, the Kappa coefficient is applied to assess the spatial distribution consistency and verify the simulation's effectiveness.

3.4.2. Scenario Design

The inertia-driven development scenario simulation forecasts future land use changes based on historical trends. Specifically, this scenario assumes that land use evolution from 2010 to 2020 will persist in the absence of external policy interventions or restrictions. Future land use patterns are thus projected by extending the past decade's change trajectories, integrating driving factors such as regional natural environments and socioeconomic dynamics to predict the extent and spatial distribution of land use transitions by 2030 [30].

The economic development scenario assumes unrestricted urban expansion. Based on the land use transition matrix from 2010 to 2020, this scenario increases the probability of conversion from cropland, grassland, and unused land to built-up areas, while maintaining constant transition probabilities between other land types [30] (Table 2).

Table 2. Economic scenario transition coefficient matrix (transition probabilities).

Original Land Type/Target Type	Farmland	Forest Land	Grassland	Water Area	Construction Land	Unused Land
Farmland	0.60	0.60	0.60	0.60	0.60	0.60
Forest land	0.03	0.03	0.03	0.03	0.03	0.03
Grassland	0.05	0.05	0.05	0.05	0.05	0.05
Water area	0.01	0.01	0.01	0.01	0.01	0.01
Construction land	0.00	0.00	0.00	0.00	0.00	0.00
Unused land	0.05	0.05	0.05	0.05	0.05	0.05

The ecological protection scenario adheres to the directives outlined in the "Beijing-Tianjin-Hebei Territorial Spatial Planning (2021–2035)" regarding ecological protection red lines and the broader ecological protection framework. In this scenario, ecological areas such as forests, grasslands, and water bodies are protected from conversion to other land types. Additionally, river systems and nature reserves are designated as restricted zones, preventing land use transformations and ensuring the preservation and sustainable development of the ecosystem [30] (Table 3).

Table 3. Ecological protection scenario transition coefficient matrix (transition probabilities).

Original Land Type/Target Type	Farmland	Forest Land	Grassland	Water Area	Construction Land	Unused Land
Farmland	0.70	0.70	0.70	0.70	0.70	0.70
Forest land	0.00	0.00	0.00	0.00	0.00	0.00
Grassland	0.00	0.00	0.00	0.00	0.00	0.00
Water area	0.00	0.00	0.00	0.00	0.00	0.00
Construction land	0.00	0.00	0.00	0.00	0.00	0.00
Unused land	0.10	0.10	0.10	0.10	0.10	0.10

3.5. Quantitative Detection of Factors Driving the Spatiotemporal Variations in Ecosystem Services

This study employed the factor and interaction detectors from the Geographical Detector package in R to quantitatively identify the underlying drivers of spatiotemporal variations in ecosystem services. The factor detector was applied to assess the spatial stratified heterogeneity of the dependent variable Y (ecosystem services) and to quantify the explanatory power of each independent variable X (natural and socioeconomic factors). The explanatory strength is expressed by the q-statistic, with higher values indicating a stronger ability of the factor to account for spatial differentiation in ecosystem services [33].

In addition, the interaction detector was utilized to reveal the joint influence of multiple factors by evaluating how their combined effects shape the spatial patterns of ecosystem services [33]. In contrast to the independent assessment conducted by the factor detector, the interaction detector uncovers synergistic or nonlinear effects among variables, thereby offering deeper insights into how multiple drivers coregulate the dynamics of ecosystem service distribution over space and time.

This approach enhances the understanding of how natural and anthropogenic factors interactively influence ecosystem services, providing a more nuanced scientific foundation for land use management and ecological planning. Compared with traditional regression-based methods, the Geographical Detector avoids issues of multicollinearity by independently evaluating the contribution of each variable, ensuring model stability and interpretability. Even under conditions of high correlation among drivers, this method remains effective in disentangling the distinct and combined impacts of individual factors on ecosystem service variation. The specific calculation formula is as follows:

$$q = (N\sigma^2 - \sum_{h=1}^{L} N_h\sigma_h^2)/N\sigma^2 \quad (2)$$

In the Formula (2), q ($0 \leq q \leq 1$) represents the degree of influence of a specific indicator on ecosystem services. A q-value closer to 1 indicates a stronger explanatory power of the indicator in relation to the spatial distribution characteristics of ecosystem services, while a q-value closer to 0 suggests a weaker explanatory power. L refers to the number of categories within the h type influencing factors, and N_h and N correspond to the number of units for the h type influencing factors and the ecosystem service density values, respectively. σ_h^2 and σ^2 represent the variances of the h type influencing factors and the ecosystem service density values, respectively.

The spatial configuration of ecosystem services is driven by multiple interacting factors. In this study, ten variables were selected from both natural and socioeconomic dimensions to investigate their influence. Among the natural environmental factors, topographic indicators—including elevation (X_1), slope (X_2), and aspect (X_3)—were employed to quantify the impact of terrain characteristics on the spatial distribution of ecosystem services [34]. Climatic variables, particularly annual precipitation (X_4), mean annual temperature (X_5),

and evapotranspiration (X_6), exert significant influence on the spatial configuration of regional ecosystem services [34].The ecological factor NDVI (X_7) reflects the trajectory of changes in ecosystem services and is a critical indicator of ecosystem evolution [35]. Socioeconomic factors, such as population density (X_8), night-time light intensity (X_9), and GDP (X_{10}), are incorporated to assess the impact of socioeconomic activities on the evolution of ecosystem services [35].

4. Results

4.1. Land Use Changes from 2000 to 2020

From 2000 to 2020, cropland consistently represented the dominant land use type within the Beijing–Tianjin–Hebei urban agglomeration, accounting for an average of 47.71% of the total area. Forest land (21.44%) and grassland (16.23%) followed as the next most prevalent land uses, while water bodies, built-up land, and unused land comprised relatively smaller proportions of the area, at 2.95%, 10.87%, and 0.80%, respectively (Figure 3). In terms of cropland conversion, between 2000 and 2010, the majority of cropland was converted into built-up land and forest land, with areas of 15,210.81 km^2 and 1819.44 km^2, respectively. However, from 2010 to 2020, the conversion trend of cropland shifted, with substantial conversion to built-up land, grassland, and forest land, covering 6868.88 km^2, 1956.69 km^2, and 1913.94 km^2, respectively.

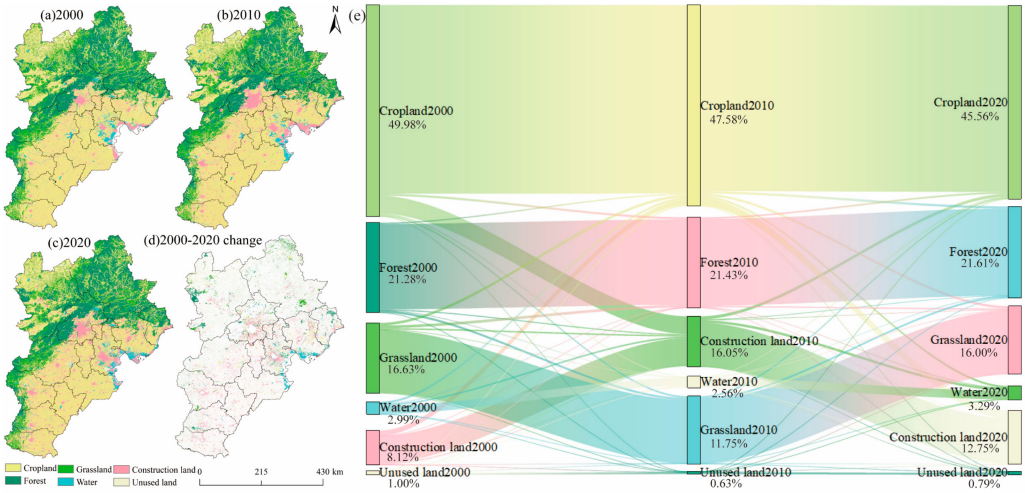


Figure 3. (**a**–**e**) Land use changes in the Beijing–Tianjin–Hebei region from 2000 to 2020. (**a**–**c**) depict the land use patterns of the Beijing–Tianjin–Hebei region in 2000, 2010, and 2020, respectively; panel (**d**) illustrates the spatial dynamics of land use transitions between 2000 and 2020; panel (**e**) presents the distribution of land conversion areas over the same period.

Throughout the past two decades, built-up land has shown a continuous expansion trend. In 2000, built-up land covered 29,438.50 km^2, or 8.12% of the total area (Figure 3). By 2010, this area had increased to 42,609.25 km^2, accounting for 11.75% of the total area. By 2020, built-up land had further expanded to 46,320.75 km^2, representing 12.74% of the total area. In terms of land conversion sources, cropland was the primary contributor to the expansion of built-up land. Between 2000 and 2010, cropland converted to built-up land accounted for 77.86% of the total cropland conversion area. However, this proportion decreased to 53.54% between 2010 and 2020. Furthermore, the areas of water bodies and unused land exhibited a notable pattern: after 2010, both bodies of water and unused land areas initially increased before subsequently decreasing.

4.2. Ecosystem Services from 2000 to 2020

From 2000 to 2020, ecosystem services in the study area exhibited distinct spatial variation (Figure 4). Carbon storage demonstrated a general increasing trend from east to west, with moderate-to-high values (average proportion: 47.65%) widely distributed in the southeastern region, while high values (average proportion: 21.41%) were concentrated in the northeastern region. Specifically, low values (average proportion: 3.01%) were primarily located along the eastern boundary of the study area, with sporadic distribution in the central region. Moderate-to-low values (average proportion: 11.72%) were predominantly found along the eastern boundary, radiating from the urban center, while moderate values (average proportion: 16.21%) concentrated in the southwestern and western peripheral regions. Between 2000 and 2020, changes in carbon storage were characterized by increases in low values (proportion: 0.34%), moderate-to-low values (proportion: 4.42%), and high values (proportion: 0.33%), while moderate values (proportion: −0.64%) and moderate-to-high values (proportion: −4.44%) exhibited a decreasing trend.

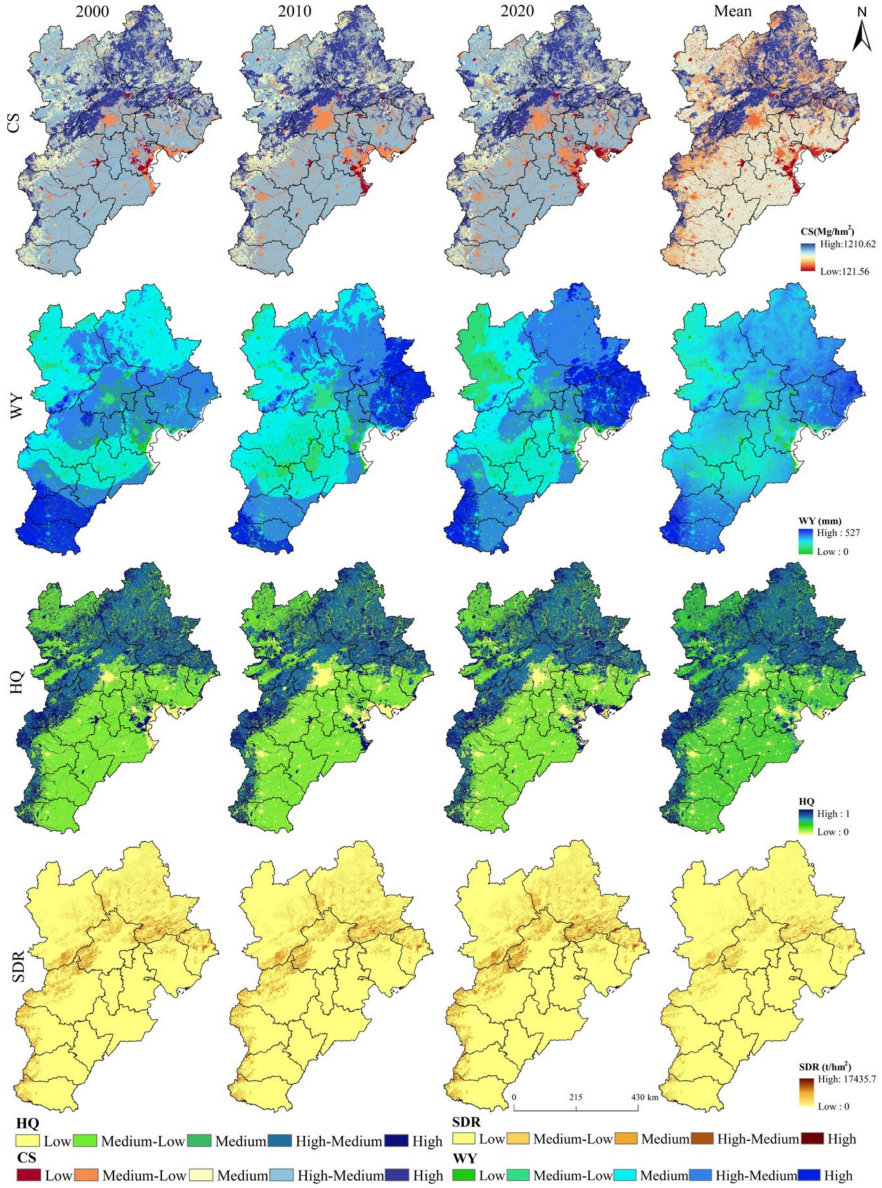


Figure 4. Spatial distribution of ecosystem service types in the Beijing–Tianjin–Hebei region from 2000 to 2020.

Water yield displayed a gradual increase from southwest to northeast, with moderate values predominating (average proportion: 36.76%), followed by moderate-to-high values (average proportion: 34.52%). Specifically, low values decreased from the central area to the southwest, with a reduction proportion of −1.73%, while moderate-to-low values gradually increased from northeast to southwest, with an increase in proportion of 10.57%. Moderate values were primarily distributed in the northwest and southern regions, with a decrease proportion of 11.73%. Moderate-to-high values shifted from the central area to the eastern region, showing an overall declining trend (proportion: −2.01%), while high values expanded mainly in the eastern region, with an increased proportion of 4.9%.

Habitat quality exhibited a spatial distribution pattern with lower values in the southeast and higher values in the west and east. Low values (average proportion: 11.26%) were concentrated in the coastal eastern and central urban areas, while moderate-to-low values (average proportion: 11.26%) were widely distributed in the southeastern region. Moderate values (average proportion: 0.80%) were sparsely distributed in the northwest, whereas moderate-to-high values (average proportion: 21.33%) formed a band stretching from northeast to southwest. High values (average proportion: 19.15%) were mainly distributed in the eastern and western peripheral regions. Over the study period, habitat quality changes were predominantly characterized by conversions between low and moderate-to-low values, with an increase in low values (proportion: 4.28%) and a decrease in moderate-to-low values (proportion: −4.25%). Moderate values and high values decreased by 0.2% and 0.23%, respectively, while moderate-to-high values increased by 0.4%.

Soil retention exhibited significant spatial variation, though temporal trends were less pronounced. Overall, low values (average proportion: 84.44%) were predominantly found in the central and central-southern regions, while other categories were mainly concentrated in the eastern, western, and western peripheral areas. Over time, low values slightly decreased (proportion: −1.81%), while other categories saw small increases, including moderate-to-low values (proportion: +0.48%), moderate values (proportion: +0.65%), moderate-to-high values (proportion: +0.47%), and high values (proportion: +0.21%). The enhancement of soil retention capacity was primarily observed in regions where forests and grasslands intersect, where these ecosystems were effectively protected, promoting the improvement of soil retention ability.

4.3. Land Use Change Simulation

By comparing the simulated land use data for 2010 in the Beijing–Tianjin–Hebei region with actual data, a Kappa coefficient of approximately 86.1% was obtained, indicating that the PLUS model is effective in simulating land use changes and is suitable for predicting land use trends for 2030 (Figure 5).

The overall spatial distribution shows that built-up areas and water bodies are predominantly concentrated in the eastern peripheral regions, interspersed with forest and grassland in the northeastern, western, and southwestern peripheral zones. Farmland is extensively distributed in the central, southern, and northwestern peripheral regions, with built-up land exhibiting a radial expansion from urban centers.

Under the inertia development scenario, farmland remains the dominant land use type, comprising 43.93% of the total area, followed by forest land (21.85%), grassland (16.02%), and built-up land (13.46%). Compared to 2020, in the inertia development scenario, farmland's proportion shows a substantial decline of 50.71%, while the proportions of water bodies and built-up areas increase by 14.09% and 22.05%, respectively. These changes are primarily observed in the peripheral regions.

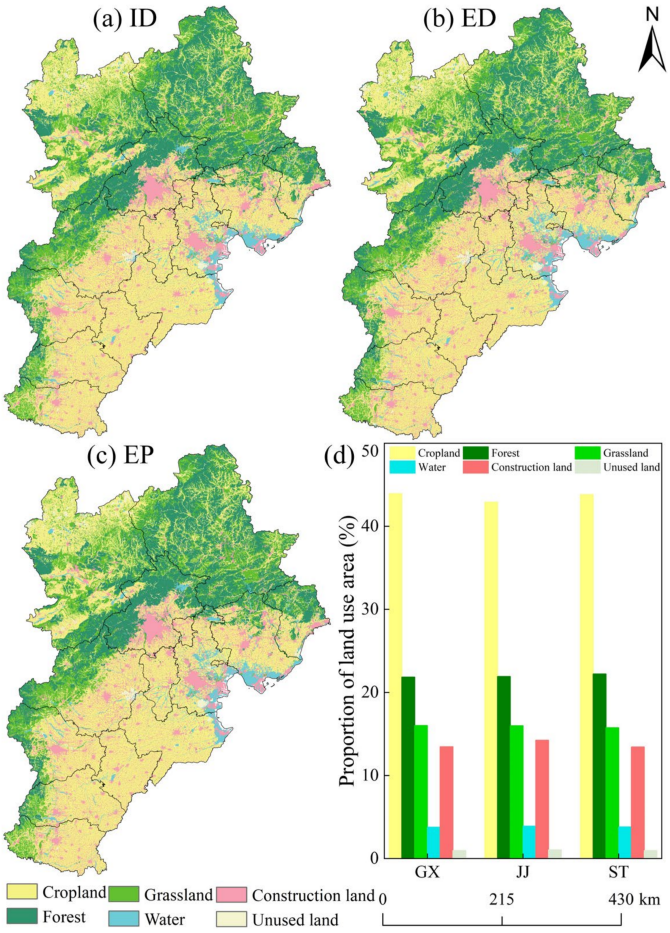


Figure 5. Spatial distribution of land use in 2030 under multiple scenarios. (**a**) Inertia development; (**b**) economic development; (**c**) ecological protection; (**d**) statistical land use types under multiple scenarios.

In the economic development scenario, farmland continues to dominate, with a share of 42.92%. At the same time, the proportions of forest land, water bodies, built-up areas, and unused land increase by 21.92%, 3.89%, 14.24%, and 1.05%, respectively. Compared to 2020, land use changes under the economic development scenario show a decrease in farmland (−49.93%) and grassland (−0.07%), while built-up areas experience a significant increase of 28.54%. These changes are mainly reflected in the expansion of built-up areas beyond the original urban boundaries, encroaching on previously existing farmland and grassland.

In the ecological protection scenario, farmland continues to be the dominant land use, with a proportion of 43.82%. Forest land, water bodies, built-up areas, and unused land see slight increases in proportion, at 22.22%, 3.80%, 13.43%, and 0.97%, respectively. Compared to 2020, land use changes in the ecological protection scenario reveal a reduction in the proportion of farmland (−43.94%) and grassland (−6.06%), while forest land increases significantly by 15.81%. The expansion of forest land is primarily observed at the edges of existing forested areas, with newly added forest regions predominantly located in areas interspersed with grassland and farmland.

4.4. Ecosystem Services Under Multiple Scenarios

Relative to 2020, ecosystem services in 2030 demonstrate modest changes across the various development scenarios (Figures 4 and 6). In all three future scenarios, carbon storage follows a consistent east-to-west gradient, with low values primarily concentrated in the eastern periphery, moderate-to-low values in the eastern and central urban centers, and moderate values in the western and southern peripheral regions. The northwest

and northeast regions display widespread moderate-to-high values, with high values predominantly appearing in the central and northeastern areas. Specifically, under the inertia development scenario, moderate-to-high values occupy the largest share (44.02%), while the economic development scenario is characterized by a higher proportion of low values (3.87%). In the ecological protection scenario, high values predominate (22.19%). Compared to 2020, in all scenarios, moderate and moderate-to-low values show slight declines, while low, moderate-to-low, and high values exhibit minor increases. Notably, the ecological protection scenario sees the most significant increase in high values (+0.59%), while the economic development scenario witnesses the greatest decrease in moderate-to-high values (−2.57%).

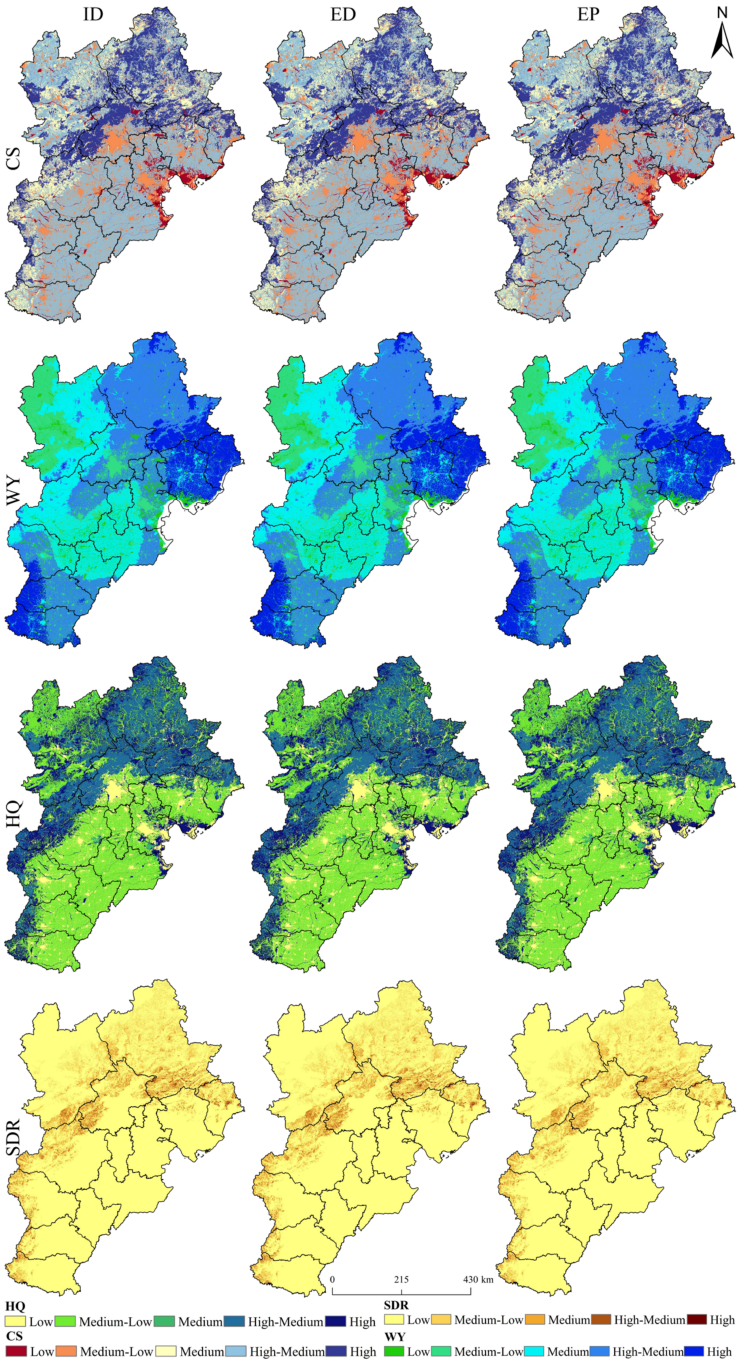


Figure 6. Spatial distribution of ecosystem service types in 2030.

The spatial distribution of water yield in the future development scenarios remains largely consistent with 2020, displaying a general increase from the southeast to the northwest. In all scenarios, the ecological protection scenario shows the highest proportion of moderate-to-high values (34.69%), while the economic development scenario is characterized by significant shares of low values (5.79%), moderate-to-low values (16.08%), and moderate values (28.76%). In contrast, the inertia development scenario exhibits the highest proportion of high values (15.37%). Relative to 2020, moderate, moderate-to-high, and high values all experience slight decreases, while low values and moderate-to-low values show small increases.

Habitat quality follows a spatial distribution pattern of lower values in the southeast and higher values in the north and west. Under the economic development scenario, both low (15.01%) and high (19.63%) values occupy substantial proportions, whereas the ecological protection scenario is marked by a higher share of moderate-to-high values (22.01%). In the inertia development scenario, moderate-to-low values dominate (43.65%). Across all scenarios, compared to 2020, there is a reduction in moderate-to-low values, with slight increases in the other categories. Particularly in the economic development scenario, moderate-to-low values decrease most sharply (−2.81%), while low values increase notably (+2.04%). In the ecological protection scenario, high values show a slight increase (+0.05%).

Soil retention displays relatively stable spatial shifts across the future development scenarios. In the ecological protection scenario, the proportion of low values is the highest (85.04%), whereas both the inertia and economic development scenarios exhibit the same proportion of high values (0.30%). Compared to 2020, changes in soil retention capacity are most prominent in the ecological protection scenario, with an increase in the proportion of low values (+1.80%), while other categories, particularly moderate values, exhibit a decreasing trend (−0.65%). This pattern suggests that the implementation of ecological protection measures has enhanced regional soil retention capacity.

4.5. The Influence of Driving Factors on the Spatiotemporal Variations of Ecosystem Services

From 2000 to 2020, the driving factors of ecosystem services in the Beijing–Tianjin–Hebei region demonstrated notable spatiotemporal variation (Figure 7). Among these, slope (X_2) consistently emerged as the primary determinant of carbon storage (q = 0.22, 0.22, 0.23), habitat quality (q = 0.36–0.42), and soil retention (q = 0.42), highlighting the enduring influence of topographic factors in regulating ecosystem functions. The annual average precipitation (X_4) was identified as a critical driver of water yield services, with q-values of 0.34, 0.38, and 0.36 in 2000, 2010, and 2020, respectively, indicating the substantial regulatory role of climate factors in water provision. Furthermore, the Normalized Difference Vegetation Index (NDVI, X_7) displayed q-values between 0.14 and 0.20 for water yield services, underscoring the vital contribution of vegetation cover to water regulation. Socioeconomic factors exhibited a progressively strengthening influence on ecosystem services. Population density (X_8) showed a pronounced effect on carbon storage in 2000 (q = 0.17) and 2020 (q = 0.21), and significantly disrupted habitat quality in 2010 (q = 0.37) and 2020 (q = 0.36). In contrast, night-time lights (X_9) exerted the least influence on soil retention ($q \leq 0.01$), suggesting a relatively weak direct impact of urbanization on this service. Overall, the trajectory of ecosystem service dynamics has shifted from being predominantly governed by topography and climate to a more integrated regulatory framework involving both natural and socioeconomic factors.

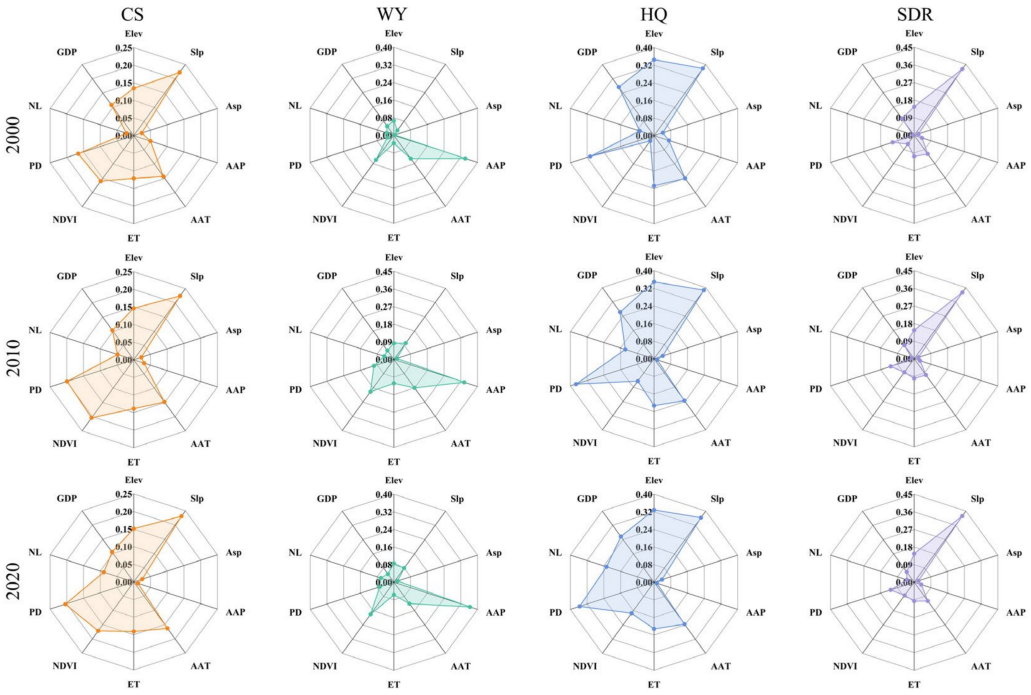


Figure 7. Explanatory power of natural environmental and socioeconomic factors on the spatial distribution patterns of ecosystem services. Note: Elev represents elevation (X_1), Slp represents slope (X_2), Asp represents aspect (X_3), AAP represents annual average precipitation (X_4), AAT represents annual average temperature (X_5), ET represents evapotranspiration (X_6), NDVI (X_7), PD represents population density (X_8), NL represents night-time light (X_9), and GDP (X_{10}). The q-values for factors X1–X10 were statistically tested and found significant at the $p < 0.05$ level.

Between 2000 and 2020, ecosystem services in the Beijing–Tianjin–Hebei region underwent notable transformations, with the influence of driving factors displaying dynamic, evolving patterns (Figure 8). Slope (X_2), as a core determinant, exhibited significant interactions with annual precipitation (X_4), annual temperature (X_5), NDVI (X_7), population density (X_8), and GDP (X_{10}), producing marked nonlinear or bidirectional enhancement effects on carbon storage, habitat quality, and soil retention services. Both annual precipitation (X_4) and NDVI (X_7) played a pivotal role in regulating soil retention and water yield services, with their interaction yielding the most pronounced effect on water yield (q = 0.49–0.54). In terms of temporal evolution, by 2000, the interaction between slope (X_2) and NDVI (X_7) (q = 0.38) emerged as the primary determinant of carbon storage, exhibiting a nonlinear enhancement, while the interaction between slope (X_2) and population density (X_8) (q = 0.43) was most influential in shaping habitat quality, demonstrating a bidirectional enhancement effect. By 2010, the interaction between slope (X_2) and NDVI (X_7) (q = 0.37) continued to serve as a key driver of carbon storage, while the influence of the slope-population density interaction (q = 0.47) further intensified its effect on habitat quality. By 2020, the interaction between NDVI (X_7) and population density (X_8) (q = 0.33) became the dominant factor influencing carbon storage, reflecting the growing role of vegetation cover and population distribution in regulating carbon stocks. Additionally, the interaction between annual precipitation (X_4) and NDVI (X_7) (q = 0.53) had the strongest impact on water yield services, emphasizing the critical role of precipitation and vegetation in the regulation of water resources.

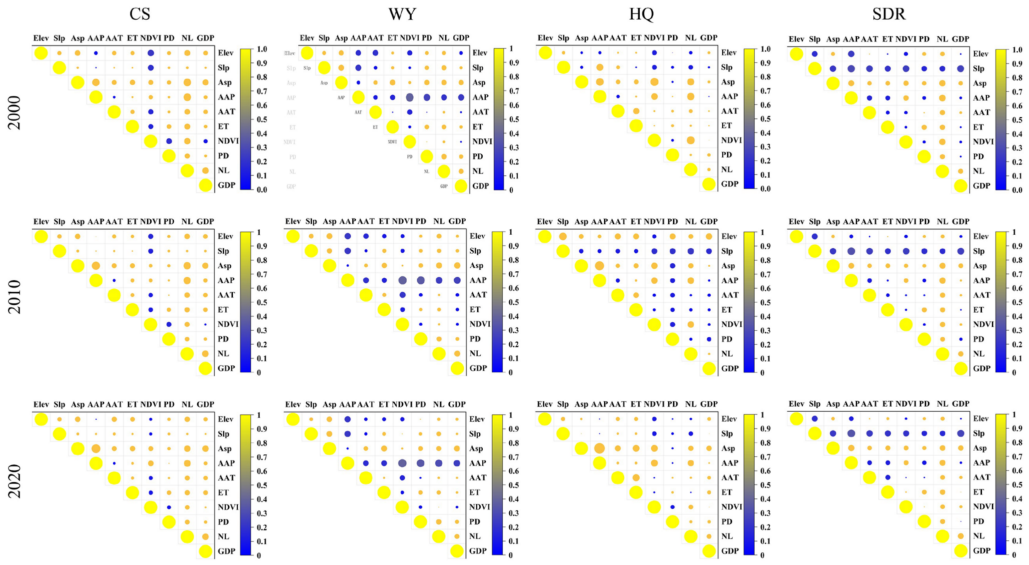


Figure 8. The interactions between natural environmental and socioeconomic factors significantly influence the spatial distribution patterns of ecosystem services, offering critical insights into their explanatory power. Note: Elev represents elevation (X_1), Slp represents Slope (X_2), Asp represents aspect (X_3), AAP represents annual average precipitation (X_4), AAT represents annual average temperature (X_5), ET represents evapotranspiration (X_6), NDVI (X_7), PD represents population density (X_8), NL represents night-time light (X_9), and GDP (X_{10}).

5. Discussion

5.1. Driving Mechanisms of Ecosystem Service Changes

The alteration of ecosystem services is influenced by a multifaceted interplay of factors, which can be broadly categorized into three primary groups: natural geographic factors, socioeconomic influences, and policy interventions. This section provides a comprehensive exploration of the driving mechanisms underlying changes in ecosystem services, with a particular focus on three key dimensions: the regulatory mechanisms of natural geographic factors, the disruptive effects of socioeconomic factors, and the regulatory influences exerted by policy interventions.

5.1.1. Regulatory Mechanisms of Natural Geographic Factors

Topographic factors (X_1, X_2, X_3) exert significant regulatory influences on ecosystem services. Elevation (X_1), through its gradient effects, shapes the spatial distribution of temperature and precipitation, thus influencing vegetation patterns and, in turn, determining regional carbon storage and habitat quality. Slope (X_2), as a critical topographic parameter, governs surface runoff and soil erosion, positioning it as a central factor in regulating soil retention and habitat quality. Aspect (X_3), by influencing solar radiation and moisture redistribution, exerts an indirect effect on water yield services. Among the climate factors (X_4, X_5, X_6), annual precipitation (X_4) and annual temperature (X_5) directly regulate vegetation productivity and hydrological cycles, acting as pivotal drivers of the spatial variation in carbon storage, water yield, and habitat quality [36]. Evaporation (X_6), through the coupling of water and energy dynamics, modulates soil moisture, thereby influencing vegetation productivity and the availability of water resources. With regard to vegetation factors (X_7), the Normalized Difference Vegetation Index (NDVI) serves as a robust ecological indicator, effectively capturing changes in vegetation cover and playing a crucial role in regulating water yield services, habitat quality, and carbon storage. However, in areas along the primary transportation corridors of Hebei Province, rural industrialization has exacerbated ecological pressures, disrupting the regulatory functions of natural factors.

Specifically, within a 120-km radius of Beijing, the degradation of forest ecosystems, along with reductions in forest cover and biomass, underscores the detrimental impact of human activities on ecosystem services.

5.1.2. Disruptive Effects of Socioeconomic Factors

Population density (X_8) and the night-time light index (X_9), as proxies for human activity intensity, significantly influence ecosystem services by driving land use/land cover (LULC) changes. The acceleration of urbanization has facilitated the conversion of natural ecosystems into artificial surfaces, markedly increasing the risk of ecological degradation [37]. Studies indicate that areas characterized by high population density and intense nighttime lighting often experience a decline in vegetation cover and heightened soil erosion, ultimately leading to reductions in carbon storage and the deterioration of habitat quality. The impact of economic development (X_{10}) on ecosystem services exhibits a dual effect. On the one hand, rapid economic growth may lead to excessive resource exploitation, resulting in soil degradation and increased habitat fragmentation. On the other hand, when guided by effective policies, ecological restoration initiatives—such as afforestation programs and wetland conservation—can enhance ecosystem service provision [38]. However, the study area faces significant challenges related to extensive land use practices, with severe forest ecosystem degradation. Statistical data indicate that per capita urban and industrial land use in Tianjin and Hebei has exceeded 160 m^2, surpassing reasonable thresholds, while unregulated rural construction has encroached upon agricultural and forested lands. For instance, between 2003 and 2011, urban construction land in Beijing expanded by 280 km^2, whereas rural collective construction land increased from 840 km^2 to 1540 km^2, with an annual growth rate twice that of urban construction. This imbalance has directly compromised Beijing's ecological security system, leading to the near disappearance of the first greenbelt and the occupation of over 50% of the second greenbelt by rural collective construction land, further exacerbating the risk of regional ecosystem service degradation.

5.1.3. Regulatory Effects of Policy Interventions

With the ongoing intensification of policy interventions, the ecological protection framework has gradually emerged as a key guiding force in shaping the trajectory of ecosystem services. This is particularly evident in the cumulative effects of major ecological initiatives and regional collaborative development policies, which are profoundly reshaping the land use patterns and the supply-demand dynamics of ecosystem services in the Beijing–Tianjin–Hebei region. Between 2000 and 2020, rapid urbanization and substantial land use changes resulted in the conversion of extensive forest, grassland, and aquatic ecosystems into built-up land, leading to a significant decline in the region's carbon sequestration capacity. Concurrently, the growing concentration of population and industrial activities has exerted sustained negative impacts on carbon storage and habitat quality, with the unchecked expansion of urban areas further intensifying habitat fragmentation, thereby becoming a critical driver of the decline in habitat quality. Since 2000, a series of major ecological restoration projects—including the Grain for Green program, coastal shelter forests, and the Three-North Shelterbelt—have been implemented, partially mitigating the region's ecological degradation. The release of the "Beijing-Tianjin-Hebei Coordinated Development Plan" marked the commencement of high-level policy coordination for regional ecological governance. This policy has reinforced the comprehensive protection and restoration of ecological spaces, playing an instrumental role in areas such as the delineation of ecological red lines, the protection of water conservation areas, and the integrated management of mountain, water, forest, farmland, lake, and grass systems. Following these

policy interventions, forest and water body areas have shown signs of restorative growth, and the functional capacity of ecosystem services has gradually improved. By 2020, four core indicators—carbon storage, habitat quality, soil retention, and water yield—had all exhibited upward trends. Notably, the implementation of major cross-regional water diversion projects, such as the South-to-North Water Diversion, has significantly optimized the spatial distribution of water resources, thereby enhancing regional water yield services and underscoring the pivotal role of policy in driving the recovery of ecosystem services [39].

5.1.4. Mechanisms of Ecosystem Service Changes Under Different Scenarios

The dynamics of ecosystem services in the Beijing–Tianjin–Hebei region exhibit marked variations under different land use scenarios, primarily driven by changes in land use structures and their spatial evolution trajectories. In the economic development scenario, urban expansion is predominantly aligned with transportation corridors and areas characterized by high nighttime light intensity, reflecting the dominant influence of socioeconomic drivers, such as GDP, population density, and anthropogenic activities. This expansion leads to substantial conversion of cropland and grassland into construction land, resulting in notable declines in carbon storage and habitat quality, particularly within the core zones of urban agglomerations. By contrast, the ecological protection scenario strictly adheres to designated ecological redlines and constrained development zones, effectively limiting the conversion of ecological land types, such as forests, grasslands, and water bodies. This scenario demonstrates the significant guiding role of policy interventions, which not only alleviate the adverse impacts of socioeconomic pressures but also enhance ecosystem functions such as water yield and soil retention, especially in the northern mountainous regions. These findings emphasize the critical role of the coupling relationship between land use trajectories and their driving forces in shaping the spatial and temporal patterns of ecosystem services. Fundamentally, the mechanisms underlying these changes are rooted in either the reduction in ecological land area or the strengthening of ecological protection, both of which directly influence ecosystem service provision [40].

5.2. Comparison with Existing Studies

This study advances the current understanding of ecosystem services by broadening the analytical scope across several dimensions, including the study region, service categories, simulation methodologies, identification of driving mechanisms, and policy orientation—thereby exhibiting both methodological innovation and practical relevance. First, in terms of spatial focus, while many previous studies have emphasized national, provincial, or major river basin scales—such as the Yangtze and Yellow Rivers [41,42]—this study centers on the Beijing–Tianjin–Hebei (BTH) urban agglomeration, a region of national strategic importance marked by pronounced heterogeneity in urban development, acute ecosystem degradation, and intensified spatial resource conflicts. As such, the BTH region provides a representative and policy-sensitive context for analyzing ecosystem service dynamics. Second, with respect to ecosystem service dimensions, most existing research has tended to focus on a single service, such as hydrological regulation [43]. In contrast, this study adopts a more integrative framework by simultaneously evaluating four core services—carbon storage, water yield, habitat quality, and soil retention—thereby facilitating a more holistic understanding of the synergistic and trade-off relationships among services under land use change trajectories. Third, regarding methodological innovation, this study diverges from traditional linear regression models [44] by employing the factor detector and interaction detector from the Geographical Detector package in R. These tools enhance the capacity to uncover both the explanatory power of individual biophysical and socioeconomic drivers and their nonlinear, interactive effects on the spatial differ-

entiation of ecosystem services, thus offering a more robust depiction of the underlying spatial complexity. Finally, from a policy perspective, this study constructs and contrasts an "economic development scenario" and an "ecological protection scenario" to explore divergent ecosystem service trajectories under alternative policy agendas. This design aligns with the evolving priorities outlined in the Beijing–Tianjin–Hebei Territorial Spatial Plan (2021–2035) and contributes valuable insights for guiding regional land use optimization and the construction of a resilient ecological security pattern.

5.3. Research Limitations

Despite the contributions of this study, several limitations should be acknowledged. First, the land use data were primarily obtained through remote sensing interpretation, which may involve uncertainties in classification accuracy and spatial resolution. Variations in the temporal and spatial resolution across different datasets may also introduce potential biases in the analysis results. Second, the spatiotemporal evolution of four key ecosystem services in the Beijing–Tianjin–Hebei region was assessed using the InVEST model. However, due to limitations in data availability, model parameters were largely adopted from existing literature rather than calibrated with field-based observations, which may affect the reliability and precision of the simulation outcomes. Moreover, although the Millennium Ecosystem Assessment (MA) provides a comprehensive framework for classifying ecosystem services, this study focused on four representative services. As a result, the broader spectrum of ecosystem service functions within the region may not be fully captured [45]. To enhance analytical accuracy and comprehensiveness, future research should incorporate field survey data to refine parameter settings and expand the range of ecosystem services analyzed. Lastly, while this study investigated the driving mechanisms of ecosystem service dynamics from both biophysical and socioeconomic dimensions, the role of cultural factors was not quantitatively addressed due to their complexity and limited measurability [46]. Future studies should aim to construct more integrative frameworks that encompass biophysical, socioeconomic, and cultural dimensions, thereby supporting more holistic and science-based decision-making in land use planning and ecosystem management.

5.4. Policy Implications

The rapid urbanization of the Beijing–Tianjin–Hebei region has intensified conflicts between land use dynamics and ecosystem services, necessitating strategic policy adjustments to ensure sustainable regional development. Thus, strengthening ecological conservation and restoration, advancing green development, and optimizing resource management have become key policy priorities.

First, enhancing ecological protection and restoration is a crucial strategy for maintaining regional sustainability. In areas with low carbon storage and degraded habitat quality, targeted conservation measures and large-scale ecological restoration initiatives should be implemented to enhance ecosystem service functions [47]. In terms of land use, optimizing land-use structure is essential to curb the excessive conversion of farmland into built-up areas while ensuring the protection of existing agricultural land. Simultaneously, the expansion of urban green spaces and ecological corridors should be promoted to maintain ecological functionality amid urbanization. Given the relatively low ecosystem service provision in plain areas, preserving farmland and natural ecosystems is critical for sustaining regional ecological stability [48]. Furthermore, integrating ecosystem service assessments into policy decision-making can provide scientific support for the coordinated development of the Beijing–Tianjin–Hebei region [49].

Second, fostering green development and promoting a low-carbon economy represent essential pathways for improving regional ecosystem services [50]. Empirical evidence suggests that socioeconomic activities, particularly in high-density urban areas, exert considerable pressure on carbon storage and habitat quality. Therefore, policy interventions should focus on facilitating low-carbon economic transitions, promoting green technologies, and implementing sustainable development strategies. To minimize ecological degradation, policies should prioritize green development in economically advanced areas, thereby enhancing carbon sequestration and ecosystem service capacities. These initiatives will contribute to the region's ecological transformation and reinforce its environmental resilience [51].

Finally, optimizing water resource management and strengthening cross-regional governance are critical for mitigating water scarcity and ecological imbalances [51]. Given the spatiotemporal variability of precipitation and water availability, implementing scientifically informed water management strategies and promoting water conservation measures are particularly essential in water-stressed areas [52]. Additionally, fostering integrated ecological governance across the Beijing–Tianjin–Hebei region can enhance water resource regulation and ecosystem service provision. Key initiatives should include wetland and farmland conservation, the promotion of water-efficient agriculture, and the acceleration of ecological restoration projects in the Yanshan-Taihang Mountain region to bolster regional ecological sustainability.

6. Conclusions

This study explores the spatiotemporal dynamics and driving mechanisms of ecosystem services in the Beijing–Tianjin–Hebei region, based on land use transitions from 2000 to 2020. The PLUS model was employed to simulate land use patterns in 2030 under three contrasting scenarios. Changes in four key ecosystem services—carbon storage, water yield, habitat quality, and soil retention—were quantified using the InVEST model, while their underlying drivers were identified through the Geographical Detector method.

The results indicate that cropland consistently dominated land use over the past two decades, accounting for 47.71% of the total area, and served as the principal source for urban expansion. The proportion of construction land increased from 8.12% to 12.74%, with 77.86% of newly developed land during 2000–2010 converted from cropland; this share declined to 53.54% during 2010–2020. Concurrently, ecosystem services generally exhibited a shift toward an increased proportion of low-to-medium value zones and a reduction in medium-to-high value areas. Notable changes included a 0.34% increase in low-value carbon storage areas and a 10.57% increase in low-to-medium water yield zones, accompanied by an 11.73% decrease in medium-value areas.

Land use trajectories and ecological responses varied markedly across scenarios. Under the business-as-usual scenario, cropland declined by 50.71%, while construction land and water bodies expanded by 22.05% and 14.09%, respectively. In the economic development scenario, cropland and grassland decreased by 49.93% and 0.07%, with construction land increasing by 28.54%. In contrast, the ecological protection scenario resulted in a 43.94% reduction in cropland and a 6.06% decrease in grassland, alongside a 15.81% increase in forest land. Under this scenario, the proportion of medium-high carbon storage areas rose by 0.59%, and medium-high water yield zones accounted for 34.69% of the region, whereas the economic scenario led to a 2.57% decline in medium-high carbon storage areas.

Driver analysis revealed that the interaction between slope (X_2) and NDVI (X_7) had the strongest explanatory power for carbon storage, underscoring the combined influence of topography and vegetation on carbon sequestration. Slope also emerged as a dominant

factor influencing habitat quality and soil retention, while annual precipitation (X_4) primarily governed water yield. Socioeconomic variables, including population density (X_8), night-time light intensity (X_9), and GDP (X_{10}), consistently exerted negative pressures on carbon storage capacity and habitat quality.

Overall, land use structure and its evolutionary trajectory play a central role in reshaping the spatial patterns of ecosystem services, with the underlying mechanism primarily driven by the reconfiguration of service supply and demand induced by reductions in ecological land or variations in protection intensity. The integrated framework of "historical evolution identification-scenario simulation-driving mechanism interpretation" proposed in this study offers both quantitative rigor and explanatory depth, rendering it well-suited to support planning efforts in regions undergoing concurrent urban expansion and ecological restoration. This framework provides a scientific foundation for optimizing territorial spatial development and enhancing ecological conservation in the Beijing–Tianjin–Hebei region, while also exhibiting strong applicability to other rapidly urbanizing areas. It offers strategic insights for improving ecosystem service provision and advancing spatial governance in similar socioecological contexts.

Future research should emphasize the localized calibration of model parameters and scenario configurations, taking into account region-specific biophysical conditions and policy priorities to enhance the regional adaptability and policy relevance of the framework. Moreover, it is imperative to strengthen the regulation and classification of ecological land use, with particular emphasis on preserving the integrity and connectivity of critical ecological function zones. The integration of ecosystem service assessments into land use planning processes is essential to systematically embed ecological values into spatial governance, thereby fostering synergistic outcomes in ecological protection and high-quality regional development.

Author Contributions: Conceptualization, S.S. and J.H.; Methodology, S.S. and J.H.; Software, S.S. and J.H.; Validation, S.S. and J.H.; Formal analysis, S.S. and J.H.; Investigation, S.S. and J.H.; Resources, J.H. and S.S.; Data curation, J.H.; Writing original draft preparation, J.H. and S.S.; Writing review and editing, S.S. and J.H.; Visualization, S.S. and J.H.; Supervision, S.S.; Project administration, S.S.; Funding acquisition, S.S. All authors have read and agreed to the published version of the manuscript.

Funding: This research received no external funding.

Data Availability Statement: The majority of the datasets used in this study are publicly available and can be accessed through public repositories. All used data repositories are cited in the main text. Land use data were derived from the Remote Sensing Image Database maintained by the Resource and Environment Science Data Center of the Chinese Academy of Sciences (http://www.resdc.cn, accessed on 8 December 2024), with a spatial resolution of 30 m. The digital elevation model (DEM) utilized in this study was the ASTER Global Digital Elevation Model (ASTER GDEM), supplied by the Geospatial Data Cloud (http://www.gscloud.cn/#page1/1, accessed on 8 December 2024), also with a resolution of 30 m. Soil data were acquired from the World Soil Database (http://westdc.westgis.ac.cn/data/611f7d50-b419-4d14-b4dd-4a944b141175, accessed on 8 December 2024), which includes characteristics such as sand, silt, and clay fractions, as well as organic carbon content, with a resolution of 1 km. Furthermore, meteorological data, encompassing precipitation and potential evapotranspiration, were obtained from the Resource and Environment Science Data Center of the Chinese Academy of Sciences (http://www.resdc.cn/, accessed on 8 December 2024).

Conflicts of Interest: The authors declare no conflicts of interest.

Appendix A

Appendix A.1 The Calculation Formula of Carbon Storage

$$C_{total} = C_{above} + C_{\text{below}} + C_{\text{dead}} + C_{\text{soil}} \quad \text{(A1)}$$

In Equation (A1): C_{total}, C_{above}, C_{below}, C_{dead}, and C_{soil}, respectively, represent total carbon (t), aboveground biomass (t), root biomass (t), carbon in dead organic matter (t), and soil organic carbon storage (t).

Acknowledging that dead organic matter carbon represents a relatively minor fraction of the carbon pool and presents challenges in data acquisition, this study has opted not to incorporate it into the analysis. Utilizing a modified carbon density formula, adjustments were made to the national carbon density data, thereby facilitating the estimation of carbon densities associated with various land use types within Beijing–Tianjin–Hebei Urban Agglomeration.

$$C_{SP} = 3.3968 \times MAP + 3996.1\left(R^2 = 0.11\right) \quad \text{(A2)}$$

$$C_{BP} = 6.798 \times e^{0.0054 \times MAP}\left(R^2 = 0.70\right) \quad \text{(A3)}$$

$$C_{BT} = 28 \times MAT + 398\left(R^2 = 0.47, P < 0.1\right) \quad \text{(A4)}$$

$$K_{BP} = \frac{C'_{BP}}{C''_{BP}} \quad \text{(A5)}$$

$$K_{BT} = \frac{C'_{BT}}{C''_{BT}} \quad \text{(A6)}$$

$$K_B = K_{BP} \times K_{BT} \quad \text{(A7)}$$

$$K_s = \frac{C'_{SP}}{C''_{SP}} \quad \text{(A8)}$$

In the equation: C_{SP} represents the soil carbon density (t·hm^{-2}) derived from annual precipitation; C_{BP} and C_{BT} represent the biomass carbon density (t·hm^{-2}) derived from annual precipitation and annual mean temperature, respectively; MAP stands for mean annual precipitation (mm); MAT stands for mean annual temperature (°C); K_{BP} and K_{BT} are the correction coefficients for precipitation and temperature factors in biomass carbon density;$C\prime$ and C'' are the carbon density data for Beijing–Tianjin–Hebei Urban Agglomeration and China, respectively; K_B and K_S are the correction coefficients for biomass carbon density and soil carbon density, respectively.

Appendix A.2 The Calculation Formula of Water Yield

$$Y(x) = \left(1 - \frac{AET(x)}{P(x)}\right) \times P(x) \quad \text{(A9)}$$

$$\frac{AET(x)}{P(x)} = 1 + \frac{PET(x)}{P(x)} - \left[1 + \left(\frac{PET(x)}{P(x)}\right)^{\omega(x)}\right]^{1/\omega(x)} \quad \text{(A10)}$$

$$PET(x) = K_{\text{c}}(l_x) \times ET_0(x) \quad \text{(A11)}$$

$$\omega(x) = Z\frac{AWC(x)}{P(x)} + 1.25 \quad \text{(A12)}$$

In the equation: $Y(x)$ represents the annual water yield (mm) for the grid cell x; $AET(x)$ represents the annual actual evapotranspiration (mm) for the grid cell x; $P(x)$ represents the annual precipitation (mm) for the grid cell x; $PET(x)$ represents the potential evapotranspiration (mm); $\omega(x)$ represents a non-physical parameter related to natural climate and soil properties; $ET_0(x)$ represents the crop (vegetation) evapotranspiration coefficient for a specific land use type in the grid cell x; $AWC(x)$ represents the available water capacity (mm) for plants; Z is an empirical constant that can be obtained based on calculations related to annual precipitation events.

Appendix A.3 The Calculation Formula of Habitat Quality

$$Q_{xj} = H_j\left(1 - \frac{D_{xj}^z}{D_{xj}^z + \mathrm{k}^2}\right) \tag{A13}$$

$$D_{xj} = \sum_{r=1}^{R}\sum_{y=1}^{Y_r}\left(\omega_r / \sum_{r=1}^{R}\omega_r\right) r_y i_{rxy} \beta_x S_{jr} \tag{A14}$$

$$i_{rxy} = 1 - \left(d_{xy}/d_{r\max}\right) \tag{A15}$$

In the equation: Q_{xj} represents the habitat quality of grid x in habitat type j; D_{xj} represents the degree of disturbance to grid x in habitat type j; k is the half-saturation constant, typically set to Q_{xj}, which is half of the maximum value obtained after a trial run; H_j represents the habitat suitability for habitat type j; R represents the stressor factor; y represents the number of grids in the raster layer for stressor factor r; Y_r represents the total number of grids occupied by stressor factors; ω_r represents the weight of stressor factor r, with values ranging from [0, 1]; r_y represents the value of stressor factor r for grid y (0 or 1); i_{rxy} represents the degree of disturbance caused by stressor factor r of grid y to habitat grid x; β_x represents the accessibility level of grid x, with values ranging from [0, 1], where 1 indicates extreme ease of access; S_{jr} represents the sensitivity of habitat type j to stressor factor r; d_{xy} represents the straight-line distance between grid x and grid y; and $d_{r\max}$ represents the maximum impact distance of stressor factor r.

Appendix A.4 The Calculation Formula of Habitat Quality

$$USLE = R \times K \times S \times L \times P \times C \tag{A16}$$

$$RKLS = R \times K \times L \times S \tag{A17}$$

$$SD = RKLS - USLE \tag{A18}$$

In the equation: $USLE$ represents the actual soil erosion amount (t); $RKLS$ represents the potential soil erosion amount (t); R is the rainfall erosivity factor (MJ·mm·hm^{-2}·h^{-1}); K is the soil erodibility factor (t·hm·h·MJ^{-1}·hm^{-2}·mm^{-1}); L and S are slope length and slope steepness factors, respectively; P is the engineering measure factor; and C is the vegetation cover and management factor.

References

1. Rinke Dias de Souza, N.; Mohn Solberg, M.K.; Hu, X.; Cherubini, F. Environmental benefits and changes in ecosystem services of climate-smart agriculture relative to conventional agriculture in Norway. *J. Environ. Manag.* **2025**, *377*, 124633. [CrossRef] [PubMed]

2. Richter, F.J.; Suter, M.; Lüscher, A.; Buchmann, N.; El Benni, N.; Feola Conz, R.; Hartmann, M.; Jan, P.; Klaus, V.H. Effects of management practices on the ecosystem-service multifunctionality of temperate grasslands. *Nat. Commun.* **2024**, *15*, 3829. [CrossRef] [PubMed]
3. Song, W.; Deng, X. Land-use/land-cover change and ecosystem service provision in China. *Sci. Total Environ.* **2017**, *576*, 705–719. [CrossRef]
4. Morton, P.; Kerkvliet, J. Lost ecosystem service costs and impact fees: Modelling scenarios for oil and gas development on U.S. public land. *J. Environ. Manag.* **2025**, *374*, 124091. [CrossRef]
5. Sheng, S.; Song, W.; Lian, H.; Ning, L. Review of Urban Land Management Based on Bibliometrics. *Land* **2022**, *11*, 1968. [CrossRef]
6. Yang, D.; Song, W. Ecological function regionalization of the core area of the Beijing-Hangzhou Grand Canal based on the leading ecological function perspective. *Ecol. Indic.* **2022**, *142*, 109247. [CrossRef]
7. Watson, K.B.; Galford, G.L.; Sonter, L.J.; Koh, I.; Ricketts, T.H. Effects of human demand on conservation planning for biodiversity and ecosystem services. *Conserv. Biol. J. Soc. Conserv. Biol.* **2019**, *33*, 942–952. [CrossRef]
8. Fu, B.; Zhang, L. Land-use change and ecosystem services: Concepts, methods and progress. *Prog. Geogr.* **2014**, *33*, 441–446.
9. Zhang, Z.; Pan, H.; Liu, Y.; Sheng, S. Ecosystem Services' Response to Land Use Intensity: A Case Study of the Hilly and Gully Region in China's Loess Plateau. *Land* **2024**, *13*, 2039. [CrossRef]
10. Liang, Y.; Song, W. Integrating potential ecosystem services losses into ecological risk assessment of land use changes: A case study on the Qinghai-Tibet Plateau. *J. Environ. Manag.* **2022**, *318*, 115607. [CrossRef]
11. Han, Z.; Song, W.; Deng, X.; Xu, X. Trade-Offs and Synergies in Ecosystem Service within the Three-Rivers Headwater Region, China. *Water* **2017**, *9*, 588. [CrossRef]
12. de Knegt, B.; Lof, M.E.; Le Clec'h, S.; Alkemade, R. Growing mismatches of supply and demand of ecosystem services in the Netherlands. *J. Environ. Manag.* **2025**, *373*, 123442. [CrossRef] [PubMed]
13. Lang, Y.; Song, W. Quantifying and mapping the responses of selected ecosystem services to projected land use changes. *Ecol. Indic.* **2019**, *102*, 186–198. [CrossRef]
14. Zhang, X.; Song, W.; Lang, Y.; Feng, X.; Yuan, Q.; Wang, J. Land use changes in the coastal zone of China's Hebei Province and the corresponding impacts on habitat quality. *Land Use Policy* **2020**, *99*, 104957. [CrossRef]
15. Kim, I.; Kwon, H. Assessing the Impacts of Urban Land Use Changes on Regional Ecosystem Services According to Urban Green Space Policies Via the Patch-Based Cellular Automata Model. *Environ. Manag.* **2021**, *67*, 192–204. [CrossRef]
16. Wang, Y.; Li, X.; Zhang, Q.; Li, J.; Zhou, X. Projections of future land use changes: Multiple scenarios-based impacts analysis on ecosystem services for Wuhan city, China. *Ecol. Indic.* **2018**, *94*, 430–445. [CrossRef]
17. Duan, X.; Chen, Y.; Wang, L.; Zheng, G.; Liang, T. The impact of land use and land cover changes on the landscape pattern and ecosystem service value in Sanjiangyuan region of the Qinghai-Tibet Plateau. *J. Environ. Manag.* **2023**, *325*, 116539. [CrossRef]
18. Felipe-Lucia, M.R.; de Frutos, A.; Comín, F.A. Modelling landscape management scenarios for equitable and sustainable futures in rural areas based on ecosystem services. *Ecosyst. People* **2022**, *18*, 76–94. [CrossRef]
19. Wang, Z.; Fu, B.; Wu, X.; Wang, S.; Li, Y.; Zhang, L.; Chen, N.; Wu, X. Exploring the interdependencies of ecosystem services and social-ecological factors on the Loess Plateau through network analysis. *Sci. Total Environ.* **2025**, *960*, 178362. [CrossRef]
20. Sharafatmandrad, M.; Khosravi Mashizi, A. Ecological succession regulates the relationship between biodiversity and supporting services in arid ecosystems. *Arab. J. Geosci.* **2021**, *14*, 1370. [CrossRef]
21. Xu, X.; Yu, J.; Wang, F. Analysis of ecosystem service drivers based on interpretive machine learning: A case study of Zhejiang Province, China. *Environ. Sci. Pollut. Res.* **2022**, *29*, 64060–64076. [CrossRef] [PubMed]
22. Qiu, J.; Yu, D.; Huang, T. Influential paths of ecosystem services on human well-being in the context of the sustainable development goals. *Sci. Total Environ.* **2022**, *852*, 158443. [CrossRef] [PubMed]
23. Joaquim Bergamo, P.; Rito, K.F.; Agostini, K.; Deodato da Silva e Silva, F.; Maues, M.M.; Rech, A.R.; Garibaldi, L.A.; Nic Lughadha, E.; Saraiva, A.M.; Tsukahara, R.Y.; et al. Identifying changes in the drivers of ecosystem services: Socioeconomic changes underlie reduced provision of pollination service. *J. Environ. Manag.* **2025**, *373*, 123466. [CrossRef]
24. Chen, T.; Huang, Q.; Wang, Q. Differentiation characteristics and driving factors of ecosystem services relationships in karst mountainous area based on geographic detector modeling: A case study of Guizhou Province. *Acta Ecol. Sin.* **2022**, *42*, 6959–6972.
25. Song, Y.; Wang, J.; Ge, Y.; Xu, C. An optimal parameters-based geographical detector model enhances geographic characteristics of explanatory variables for spatial heterogeneity analysis: Cases with different types of spatial data. *Giscience Remote Sens.* **2020**, *57*, 593–610. [CrossRef]
26. Wang, H.; Liu, L.; Yin, L.; Shen, J.; Li, S. Exploring the complex relationships and drivers of ecosystem services across different geomorphological types in the Beijing-Tianjin-Hebei region, China (2000–2018). *Ecol. Indic.* **2021**, *121*, 107116. [CrossRef]
27. Peng, S.; Ding, Y.; Liu, W.; Li, Z. 1 km monthly temperature and precipitation dataset for China from 1901 to 2017. *Earth Syst. Sci. Data* **2019**, *11*, 1931–1946. [CrossRef]
28. Didan, K. MOD13A3 MODIS/Terra Vegetation Indices Monthly L3 Global 1km Sin Grid V006 [Data Set]. 2015. Available online: https://ladsweb.modaps.eosdis.nasa.gov/missions-and-measurements/products/MOD13A3 (accessed on 8 December 2024).

29. Zhang, L.; Ren, Z.; Chen, B.; Gong, P.; Xu, B.; Fu, H. A Prolonged artificial nighttime-light dataset of China (1984–2020). *Sci. Data* **2024**, *11*, 414. [CrossRef]
30. Chen, J.; Fu, H.; Chen, S. Multi-Scenario Simulation and Assessment of Ecosystem Service Value at the City Level from the Perspective of "Production–Living–Ecological" Spaces: A Case Study of Haikou, China. *Land* **2023**, *12*, 1021. [CrossRef]
31. Wang, Z.; Song, W.; Yin, L. Responses in ecosystem services to projected land cover changes on the Tibetan Plateau. *Ecol. Indic.* **2022**, *142*, 109228. [CrossRef]
32. Fang, Y.; Hu, R.; Meng, F.; Luo, M.; Sa, C.; Bao, Y.; Lei, J.; Chao, L. Spatiotemporal Dynamics of Ecosystem Service Balance in the Beijing-Tianjin-Hebei Region and Its Ecological Security Barrier with Inner Mongolia. *Atmosphere* **2024**, *15*, 76. [CrossRef]
33. Yang, L.; Liu, Y.; Liu, Y.; Liu, R. Spatial-temporal dynamics and drivers of ecosystem service interactions along the Yellow River area in Shaanxi Province. *J. Clean. Prod.* **2025**, *496*, 145095. [CrossRef]
34. Liu, R.; Li, L.; Guo, L.; Jiao, L.; Wang, Y.; Cao, L.; Wang, Y. Multi-scenario simulation of ecological risk assessment based on ecosystem service values in the Beijing-Tianjin-Hebei region. *Environ. Monit. Assess.* **2022**, *194*, 434. [CrossRef]
35. Shen, J.; Li, S.; Liu, L.; Liang, Z.; Wang, Y.; Wang, H.; Wu, S. Uncovering the relationships between ecosystem services and social-ecological drivers at different spatial scales in the Beijing-Tianjin-Hebei region. *J. Clean. Prod.* **2021**, *290*, 125193. [CrossRef]
36. Braun, D.; de Jong, R.; Schaepman, M.E.; Furrer, R.; Hein, L.; Kienast, F.; Damm, A. Ecosystem service change caused by climatological and non-climatological drivers: A Swiss case study. *Ecol. Appl. A Publ. Ecol. Soc. Am.* **2019**, *29*, e01901. [CrossRef]
37. Schirpke, U.; Tasser, E.; Borsky, S.; Braun, M.; Eitzinger, J.; Gaube, V.; Getzner, M.; Glatzel, S.; Gschwantner, T.; Kirchner, M.; et al. Past and future impacts of land-use changes on ecosystem services in Austria. *J. Environ. Manag.* **2023**, *345*, 118728. [CrossRef]
38. Li, Z.Z.; Hu, B.; Qin, Y.; Cheng, X. Drivers of spatiotemporal disparities in the supply-demand budget of ecosystem services: A case study in the Beijing-Tianjin-Hebei urban agglomeration, China. *Front. Environ. Sci.* **2022**, *10*, 955876. [CrossRef]
39. Qu, J.; Jiang, J.; Yan, T.; Li, Y.; Tian, R.; Wang, L. Evolution of groundwater ecosystem service value in the receiving areas of Beijing-Tianjin-Hebei around the opening of the Middle Route Project of South-to-North Water Diversion. *Acta Geophys.* **2024**, *72*, 2743–2758. [CrossRef]
40. Li, Q.; Shi, X.; Zhao, Z.; Wu, Q. Multi-Scenario Simulation of Ecosystems Based on Adaptive Restoration to Promote Human–Nature Harmony: A Case Study of Loess Hills Micro-Watershed. *Land* **2024**, *13*, 233. [CrossRef]
41. Dang, L.; Zhao, F.; Teng, Y.; Teng, J.; Zhan, J.; Zhang, F.; Liu, W.; Wang, L. Scale dependency of trade-offs/synergies analysis of ecosystem services based on Bayesian Belief Networks: A case of the Yellow River Basin. *J. Environ. Manag.* **2025**, *375*, 124410. [CrossRef]
42. Zheng, Y.; Sang, X.; Li, Z.; Zhang, S.; Chang, J. Ecological services value of 'natural-artificial' water cycle: Valuation method and its application in the Yangtze River Basin of China. *Ecol. Indic.* **2024**, *158*, 111324. [CrossRef]
43. Xiao, Y.; Xiao, Q.; Ouyang, Z.; Qin, M. Assessing changes in water flow regulation in Chongqing region, China. *Environ. Monit. Assess.* **2015**, *187*, 362. [CrossRef]
44. Zhang, Z.; Tong, Z.; Zhang, L.; Liu, Y. What are the dominant factors and optimal driving threshold for the synergy and tradeoff between ecosystem services, from a nonlinear coupling perspective? *J. Clean. Prod.* **2023**, *422*, 138609. [CrossRef]
45. Li, Q.; Li, D.; Wang, J.; Wang, S.; Wang, R.; Fu, G.; Yuan, Y.; Zheng, Z. Spatial heterogeneity of ecosystem service bundles and the driving factors in the Beijing-Tianjin-Hebei region. *J. Clean. Prod.* **2024**, *479*, 144006. [CrossRef]
46. Valenca Pinto, L.; Inacio, M.; Bogdzevic, K.; Gomes, E.; Pereira, P. Factors affecting the use of cultural ecosystem services in Lithuanian coastal area. *Ocean. Coast. Manag.* **2024**, *251*, 107095. [CrossRef]
47. Bai, Y.; Ali, M.; Zhou, Y.; Yang, S. Quantifying marginal utilities of ecosystem services for sustainable management. *J. Clean. Prod.* **2024**, *470*, 143353. [CrossRef]
48. Xiao, R.; Lin, M.; Fei, X.; Li, Y.; Zhang, Z.; Meng, Q. Exploring the interactive coercing relationship between urbanization and ecosystem service value in the Shanghai–Hangzhou Bay Metropolitan Region. *J. Clean. Prod.* **2020**, *253*, 119803. [CrossRef]
49. Fang, G.; Sun, X.; Liao, C.; Xiao, Y.; Yang, P.; Liu, Q. How do ecosystem services evolve across urban–rural transitional landscapes of Beijing–Tianjin–Hebei region in China: Patterns, trade-offs, and drivers. *Landsc. Ecol.* **2023**, *38*, 1125–1145. [CrossRef]
50. Hysa, A.; Lowe, R.; Geist, J. Ecosystem services potential is declining across European capital metropolitan areas. *Sci. Rep.* **2024**, *14*, 8903. [CrossRef]
51. Jian, S.; Ding, X.; Yu, X. Land use simulation for synergistic water and soil ecosystem services. *Acta Ecol. Sin.* **2024**, *44*, 9470–9484.
52. Wu, A.; Zhang, J.; Zhao, Y.; Shen, H.; Guo, X. Simulation and Optimization of Supply and Demand Pattern of Multiobjective Ecosystem Services—A Case Study of the Beijing-Tianjin-Hebei Region. *Sustainability* **2022**, *14*, 2658. [CrossRef]

Disclaimer/Publisher's Note: The statements, opinions and data contained in all publications are solely those of the individual author(s) and contributor(s) and not of MDPI and/or the editor(s). MDPI and/or the editor(s) disclaim responsibility for any injury to people or property resulting from any ideas, methods, instructions or products referred to in the content.